Aalto-yliopisto
Insinööritieteiden
korkeakoulu

Farid Ullah

Early Age Autogenous Shrinkage and Long-term Drying Shrinkage of Fibre Reinforced Concrete.

Thesis submitted in partial fulfillment of the requirements for the degree of Master of Science in Structural Engineering and Building Technology.

Espoo 26.09.2017
Supervisor: Professor of Practice. Jouni Punkki
Advisor: Professor of Practice. Jouni Punkki

Aalto University
School of Engineering

Aalto University, P.O. BOX 11000, 00076 AALTO
www.aalto.fi

Abstract of master's thesis

Author Farid Ullah

Title of thesis Early Age Autogenous Shrinkage and Long-term Drying Shrinkage of Fibre Reinforced Concrete

Degree program Structural Engineering and Building Technology

Major/minor Structural Engineering/Construction Management **Code** R3001

Thesis supervisor Professor of Practice. Jouni Punkki

Thesis advisor Professor of Practice. Jouni Punkki

Date 26.09.2017 **Number of pages** 60+6 **Language** English

Abstract

The role of fibres against cracking in concrete because of volumetric deformations has become popular over the years. Various researchers have reported the crack-control benefits of fibres in both fresh and hardened concrete. The volumetric changes of concrete are broadly divided into early-age and long-term deformations. The volume change in concrete begins with the hydration reactions when water is mixed with cement. Contrary to the long-term shrinkage deformations, the early-age deformations are usually ignored in design of concrete structures because of lesser magnitude. In autogenous conditions, capillary pressure in pores result in significant deformation, thus creating potential for cracking. Especially in concretes with low water-to-cement ratio, capillary pressure can cause significant autogenous shrinkage deformations. In the absence of moisture evaporation, hydration reactions cause noteworthy thermal heating, followed by cooling in fresh concrete. Moreover, thermal deformations manifest in the form of expansion and contraction in fresh concrete, which produce internal stresses that increase the vulnerability of cracking.

The aim of this thesis was to study the effects of different types of fibres on the early-age autogenous and long-term drying shrinkage deformations of concrete. A test setup called Schleibinger Bending-drain was used to record early-age (2days) autogenous deformations of fresh concrete immediately after mixing. The test results were used to study the physical processes controlling different stages of the early-age autogenous deformation in relation to the effect of fibres and concrete composition. The early-age autogenous deformations in Plus and SR cement concrete were significantly reduced by the use of 0.38% by volume of steel and plastic fibres as compared to plain concrete. However, 0.38% by volume of plastic and glass fibres used in White cement concrete had a small effect on the early-age autogenous deformations. Other than fibres, the factors affecting the early-age autogenous deformations were different cement types (hydration heat) and the shrinkage-reducing admixture. The lesser amount of bleed-water in White cement concrete resulted in large magnitude early-age autogenous deformation. The use of fibres at 0.38% by volume did not have a prominent effect on the 56 days unrestrained drying shrinkage deformation. The general opinion that fibres allow more moisture escape by bridging the pores could not be established as similar average water loss (kg/m^3) was recorded for both the plain and fibre reinforced concrete mixtures. Moreover, the magnitude of early-age autogenous deformations was approximately 19%, 22% and 51% of the total combined deformations (early-age and long-term) for Plus, SR and White cement concretes, respectively.

Keywords Autogenous shrinkage, Drying shrinkage, Concrete cracking, Fibre reinforced concrete, Thermal deformation, capillary pressure, water-to-cement ratio, hydration heat, Bending-drain.

Acknowledgement

By the grace of Allah, this Master's thesis work concludes an amazing journey, at Aalto University. This work was done with funding from Aalto University School of Engineering's Department of Civil Engineering, during December 2016 – May 2017.

I would like to express my gratitude to my thesis supervisor and advisor, Professor of Practice Jouni Punkki for his constant support and belief in me. This work was not possible without his able guidance and encouragement. I would also like to acknowledge the invaluable assistance of Manager of Testing Hall Veli-Antti Hakala, laboratory manager Jukka Piironen and Laboratory Technician Pertti Alho of the Testing Hall of Structural Engineering. Their support and knowledge enabled me to complete the experimental work safely and timely.

I would also thank my parents and family, whose love and support are a source of inspiration for my life endeavors. Finally, I would thank my friends and colleagues who have supported me throughout my studies.

Espoo 26.09.2017

Farid Ullah

Farid Ullah

Contents

List of Tables

List of Figures

1 Introduction

With the advancements in concrete materials and production technology, concrete is now tailor-made to provide such precise properties as are required for a particular application. Fibres are added in the concrete with the purpose of improving strength and durability. Fibres act through frictional effects and mechanical/chemical bond between fibres and matrix. The knowledge of fibre reinforced concrete, based on theoretical solutions and experimental findings is rich and quite large. However, practical applications are limited. Insufficient development of standards for fibre use and high cost of fibre reinforced concrete are major hurdles in this area. Concrete being weak in tension is susceptible to cracking even under self-weight if proper care is not taken. Fibres addition offsets the stresses and prevents or limits cracking of already existing cracks. The lack of resistance to initiation and propagation of cracks in young concrete is as serious a challenge as the lack of strength or stiffness in hardened concrete.

Concrete, a heterogeneous material, is formed by a series of chemical reactions between raw materials. The constituents usually include a binder (cement), water, sand, aggregate and admixtures. The chemical reactions that start from mixing of raw ingredients form a gel paste products in which the aggregates are packed. Volume instability such as shrinkage, due to environmental and structural factors is an acceptable process and it is catered for in concrete design and construction. The volumetric changes in concrete occur as soon as hydration takes place. Large amount of heat released during the hydration reactions is a major cause of evaporation of water from the concrete. Water is also utilized internally during the hydration process. Therefore, volumetric changes in the concrete start right away form fresh fluid stage during the setting process and may continue for a long time as the concrete keeps on drying.

In reality, structural concrete is restrained by adjacent structural members, due to which tensile forces gradually build up. This build-up of internal stresses may lead to the development of cracks, increase in deflection of concrete members and widening of existing cracks. However, either reinforcements or adjoining concrete members restrain the deflections. Concrete is weak in tension, and reinforcement is added to improve tensile and flexural properties. Furthermore, concrete is brittle as well, cracks occurrence is considered normal. Cracks form up whenever the deformations-induced tensile stresses in the concrete exceed its tensile capacity. More often than less, shrinkage is at the origin of crack formation in concrete (Alvaredo, 1993; Alvaredo & Wittmann, 1995; Wittmann, 1985). The cracks in concrete may give easy access to ingress of harmful agents and moisture inside concrete, which are potential agents for corrosion of steel reinforcement. Immediate curing few hours after the placement of concrete has been long used to avoid shrinkage in plastic stage of concrete.

ACI 116R, Cement and Concrete Terminology defines fibre reinforced concrete (FRC) as *concrete containing dispersed randomly oriented fibres*. The use of steel fibres as dispersed reinforcement for concrete was proposed first by Romualdi in 1963 and 1964 (Brandt, 2008; Zollo, 1996). Brandt (2008) stated that fibres have been used since biblical times in order to strengthen brittle materials (Brandt, 2008). Examples can be seen as straw and horsehair mixed with clay to form bricks and floors. Over the years, the concept of dispersed fibres in cement-based composites has resulted in hundreds of research publications, books, and successful commercial applications and products for the buildings and civil engineering structures all over the world. From cement replacement to the use of admixtures, various kind of concretes have been developed to modify the properties of concrete in fresh and hardened state.

Concrete is also known as the man made rock. It is the single most widely used material in the built environment due to readily available raw materials and ability to be molded in the desired shape.

Scientists and academia has worked over the years to improve the properties of concrete to make it more sustainable, durable and economical. The age related issues such as design-life make factors such as long-term drying shrinkage a key issue of design. Fibre reinforced concrete (FRC) is an example of such a special type of concrete, which has the potential of addressing the need of durability of structures by ensuring cracks-free concrete. The tensile capacity of the concrete at early stages is lowest making it vulnerable to cracking. The enhanced cracking resistance is considered the most important feature of FRC with no standard measuring rationale. Therefore, experimental work is relied upon to evaluate the efficacy of fibres in resisting cracking of concrete.

2 Background

Volumetric deformation of concrete results from many contributing factors. This section covers the scientific contributions to explain these factors and their implications. Excessive shrinkage deformation may result in cracking of concrete members, which is detrimental to the durability of concrete structures. Loss of water over long duration due to drying is a common cause of shrinkage. However, shrinkage deformation may also occur when the loss of water is prevented. This type of shrinkage is called *autogenous shrinkage deformation.* The concretes with low water-to-binder ratio are more susceptible to shrinkage deformation. The concrete at early-age is still moist and gaining strength. Cracking or high probability of cracking in fresh concrete is a great concern and has been the focus of recent research in this field.

Concrete composites with discontinuous, discrete, uniformly dispersed suitable fibres are known as Fibre Reinforced Concretes (FRC). Control of shrinkage deformation has been highlighted in literature as a major benefit of fibres among other structural benefits of FRC. Various researchers have established the benefits of fibres in concrete shrinkage through laboratory experiments. A brief summary listing the effect of fibres on the concrete shrinkage deformation has been included in Table 10 of Section 2.4.2. Fibres make the concrete composites more durable by limiting the crack-width and dispersing major cracks into a network of micro-cracks. Despite the fact that the mechanism behind the effect of fibres on the free shrinkage and water evaporation is not clear, the addition of fibres to the cementitious composite is a promising prospect to limit the effects of shrinkage.

Shrinkage deformation of concrete may be summed up as volume instability of the water-cement paste. Changes occurring inside this paste portion govern the overall phenomenon of shrinkage deformation. Loss of water to surroundings (drying) or the use of water internally during hydration (autogenous), both result in overall deformation.

2.1 Stages of Shrinkage Deformation

Shrinkage deformation can be divided into many types based on the factors affecting the volume stability of concrete. However, overall deformation of concrete occurs in two phases, early age and long-term deformations. Figure 1 shows the stages and types of shrinkage deformation in concrete composites. The first early stage shrinkage deformation occurs when concrete is setting and starts hardening in the first 24 hours. In addition, long-term shrinkage deformation is defined as the deformation from and after the age of 24 hours (Holt, 2001). These age-based classifications of shrinkage deformation include many types of changes attributed to autogenous and drying deformation. The age-based classification also emphasizes that concrete deformation is a function of various factors.

First 24 hours of fresh concrete represent a period of fluidity followed by the loss of workability as the concrete stiffens and finally becomes rigid with hardening (Holt, 2001). There is a transition when the concrete changes from a fluid to rigid state. *This changing over process in which concrete develops the ability to stand as skeleton without much strength is called setting*.

In the *liquid stage* when concrete is placed and finished, excess bleed water moves to the surface while large aggregates settle. The *skeleton formation stage* occurs about two to three hours after mixing of cement and water (Holt, 2001). Concretes with higher amount of water (w/c) take longer to set. Similarly, admixtures of different types affect the setting time. Ambient conditions such as temperature is also another key factor that controls setting process. Concrete sets faster and gains strength at a higher rate at high temperatures. As soon as a loose internal skeleton is formed in the fresh concrete, the rate of early age deformation reduces. With the onset of *hardening*, deformation rate slows down even more, as the internal structure becomes strong enough to withstand volumetric

changes. Holt (2001) validated the phenomenon that it starts 2 hours after initial setting in her research (Holt, 2001). If the matrix is not strong enough at this, cracks may form easily.

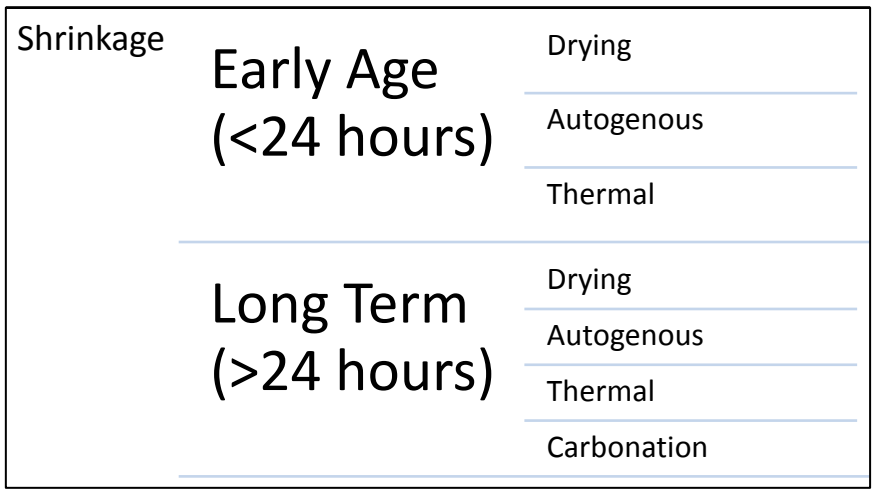

Figure 1 Division of shrinkage stages and types. (Holt, 2001)

2.1.1 Early Age Autogenous Deformation

Autogenous deformation is a result of the internal chemical reactions of concrete raw materials without moisture loss to the surroundings. The various stages of hydration manifest themselves in different stages of volumetric deformations of concrete. The deformation rate keeps on changing from the time of mixing water and cement, during setting and then hardening. There is at times greater emphasis on the early age deformation effects as the concrete is relatively weak and susceptible to cracking. The driving forces for the early-age autogenous deformation could be summed up as:

- Internal reactions of the mixture components.
- Temperature and relative humidity (ambient conditions).

Loss of water, either due to evaporation or due to consumption in the hydration gives rise to change of pore water configuration in the capillary pores. This type of deformation, with moisture loss due to evaporation, at an early age is known as plastic deformation. During the very first hours of mixing, concrete is liquid and acts as a plastic. In high-performance concretes, which has less free water, autogenous shrinkage deformations (when water is drawn from pores for hydration) is an important part of the total concrete shrinkage (Barr & El-Baden, 2003; Saje, et al., 2003). Due to less amount of free water in high-performance concrete, water is drawn from the pores that develops a pore pressure, which becomes a driving force for shrinkage deformation.

In this work, early-age autogenous deformations do not necessarily mean shrinkage deformation. Interplay of contracting forces such as capillary pressure and swelling forces such as thermal heating during early hydration, control the overall nature of the early-age autogenous deformations.

2.1.2 Long-term Shrinkage

Long-term drying shrinkage in this work is considered to start approximately twenty-four hours after mixing of water and cement. The molds or formwork is removed from concrete about this time. Drying shrinkage may continue for years in the concrete structure and as such, standard guidelines exist for its calculation. Apart from the raw materials and environmental factors, geometry (shape and size) are also responsible in determining the moisture loss. Quantitative

explanations like volume-to-surface area ratio accounts for the size and shape of concrete in long-term shrinkage measurements. A higher volume-to-surface ratio exhibits lesser shrinkage (Mindess & Young, 1981). To demonstrate the effect of volume-to-surface ratio, consider a comparison of a T-beam and a solid rectangular beam with different volume-to-surface ratios. Let, the width and height of the two beams be same. In this case, due to shorter diffusion path, T-beam will have faster drying with less ultimate shrinkage. Evidently, slender members dry up faster than thicker cross-sections.

There is lack of correlation between the early-age deformations and long-term shrinkage deformations, which makes the volumetric deformation studies of concrete difficult. Furthermore, the study of the early-age deformation is a greater challenge as the concrete is fluid and the body of concrete may move to accommodate the deformation changes. Long-term shrinkage effects could be comparable with the early age autogenous effects in the form of their absolute magnitudes. Hence, the total shrinkage of a concrete specimen could be greatly influenced by the early age effects. Any cracks forming at an early age could ultimately control the durability of concrete works. However, it is stated the first day curing conditions do not affect the long-term shrinkage effects (Holt, 2001). Drying of concrete is a slow process and may continue for years before moisture equilibrium is achieved even in layers near the surface of concrete members. Outer layers dry quicker and moisture gradient exists. Drying shrinkage is complicated further when the moisture gradient within concrete is considered. Factors such as monolithic nature of concrete elements, moisture gradient, creep, tensile strength, strain softening, and dimensions of members and modulus of elasticity all affect the shrinkage (Wittmann, et al., 2009). Stress free shrinkage does not exist in practice as concrete structures are under service in reality. It is desirable sometimes to measure the shrinkage effects in the near surface zones in infinitesimal layers to study drying effects with simplicity.

Despite the difficulties, standard practices exist to measure or estimate long-term shrinkage of concrete mixtures in the laboratory. In addition, prediction models are also be used to calculate the long-term shrinkage. The CEB/FIP model code for concrete structures gives following equation for the calculation of total shrinkage or swelling strains $\varepsilon_{cs}(t,t_s)$ [1990]:

$$\varepsilon_{cs}(t, t_s) = \varepsilon_{cso}\beta_s(t - t_s) \quad (1)$$

where: ε_{cso} = notional shrinkage coefficient (depends on mean compressive strength of concrete, type of cement and ambient conditions),
β_s = coefficient to describe the development of shrinkage with time,
t = age of the concrete (days)
t_s = the age of concrete (days) at the beginning of shrinkage or swelling.

2.2 Types of Shrinkage

2.2.1 Autogenous

With no moisture transfer to the surroundings, the external volume change of concrete or cement paste is called autogenous shrinkage. Cement hydration reactions are great factor causing autogenous shrinkage as it generates driving forces for autogenous shrinkage. Voids are generated as the products of hydration are said to occupy lesser space than raw materials and an overall shrinkage occurs. Therefore, autogenous shrinkage is part of the chemical reactions that occur between the raw materials of concrete. The outcome of the chemical reactions that form up the hydration products translates as macroscopic shrinkage deformation. This can be measured as a linear change of length. Unlike drying shrinkage, it cannot be controlled by curing or casting techniques.

Various names have been given to this type of shrinkage deformation. They include autogenous deformation, volume contraction, Le Chatelier shrinkage, bulk shrinkage, indigenous shrinkage, self-desiccation shrinkage, and autogenous volume change (Justnes, et al., 1996). It was generally associated with concrete composites of low water-to-cement (w/c) ratio. Therefore, it was ignored in earlier times as the w/c ratio was usually high. With the advent of high strength and ultra-high strength concrete mixtures and use of admixtures, concrete with low w/c ratio became possible. And with less free water (w/c) in the mixture, autogenous effects need extra care. In this work, the autogenous deformation occurrence has been considered in the early stage (first 24 hours) during the liquid phase, skeleton formation phase and hardening phase.

In *Liquid stage,* chemical shrinkage reduces the volume of the mix and voids are created. So, initially autogenous effects are purely chemical. As the hydration goes on, free water is utilized and *self-desiccation* may occur which is localized drying of internal pores of concrete. The stiffening continues and a weak *skeleton* is formed, which is able to resist the tensile effects of shrinkage deformation. When the fresh concrete has gained considerable strength, capillary pressure starts rising in the pores, which takes over as the cause of shrinkage. As described by Radocea, contraction of the cement paste of concrete is caused by the stress on the capillary pore walls as the water is lost from pores and meniscus is pulled down into the pores (Holt, 2001). The meniscus surface moves between the pores to keep this pressure mechanism until a *breakthrough* pressure or *critical* pressure reaches. After this, the pore water is redistributed notwithstanding the continuous suction or rising. It should be noted that capillary pressure does not develop and increase if there is bleed water present on the surface of fresh concrete.

This means that the driving factors for the autogenous shrinkage keep evolving with the hydration reactions as the concrete gains strength. The so-called *skeleton formation* starts at approximately 5 hours form the mixing. On the second day after mixing, placing and finishing concrete, if the concrete is not properly cured, *self-desiccation* is a major influence of shrinkage as water becomes lesser in the concrete. Good curing practices are essential to avoid this process and to ensure complete hydration of the free cement in the mix. The rate of self-desiccation is different for concretes with different water-to-binder ratios. Free cement draws water from the pores lowering the relative humidity. If a mineral admixture like silica fume is used, the pore structure becomes finer. In this way, the pore water becomes more accessible for hydration. In this case, the relative humidity decreases fast causing autogenous shrinkage deformation because of self-desiccation (Kinuthia, et al., 2000).

2.2.2 Chemical

Chemical shrinkage is based on the initial and final volumes of hydration reactants and products. The general equation for chemical shrinkage is given below (Paulini, 1996):

$$CS = \frac{(V_c + V_w) - V_{hy}}{V_{c_i} + V_{w_i}} * 100 \quad (2)$$

where: CS = chemical shrinkage,
V_{Ci} = volume of cement before mixing,
V_C = volume of hydrated cement,
V_{Wi} = volume of water before mixing,
V_W = volume of reacted water, and
V_{hy} = volume of hydrated products.

It is important to look in to the individual cement components to track the chemical shrinkage effects in the cement paste or concrete. The clinker compounds react with water in an exothermic reaction causing a decreased volume of the reaction products, chemical shrinkage. Therefore, the chemical

composition of the cement is important in determining chemical effects of the autogenous shrinkage.

2.2.3 Carbonation

Carbon dioxide reacting in the presence of pore moisture with cement paste forms carbonates. This reduces the overall pH of the concrete making reinforcements vulnerable to corrosion. The products of rusting occupy greater volume than hydration products. They cause expansion and eventually cracking and spalling in the concrete members (Kosmatka & Panarese, 1988). Ingress of CO_2 depends upon the concrete density, pore sizes and exposure environment. Carbonation itself is cause of other types of failures of concrete and manifests in the form of spalling and cracking.

2.2.4 Drying

Loss of water from concrete resulting in the volume reduction refers to drying shrinkage. Bleed water evaporates to the surrounding when concrete consolidates upon placement. Drying continues even after bleed water has evaporated. A capillary pressure builds up in the pore structure of the fresh concrete due to evaporation as water from interior of the concrete is pulled towards the surface. Surface cracking may occur in cases of early-age drying if water is not replenished with curing.

The *internal pore structure* is said to control the drying process of concrete. The rising capillary pressure is dependent on *internal pore spaces*. Cement paste becomes denser with lower water-to-cement (w/c) ratios. The development of pore pressure occurs as water escapes first from the large pores first. If the rate of evaporation exceeds the rate of rising bleed water to surface, pores near the surface inside the concrete start loosing water. This is where drying shrinkage begins.

In a situation when the amount of evaporating water exceeds the bleed water rising from within the concrete, the water surface drops inside the concrete body. At this point, the surface of the concrete can be considered as dry. This process develops a water pressure inside the pores and in turn causes a capillary force inside the concrete matrix. The pressure difference between the inside and the outside of the meniscus is often called the *Laplace pressure*. The capillary force is described as a function of radius of curvature of the resultant meniscus between the water and air. The suction force *s* given by the Laplace equation is as follows (Janz, 2000):

$$s = \frac{2\sigma}{r} \tag{3}$$

where: s = suction pressure (Pa),
σ = surface tension of air-water interface (~0.074 N/m), and
r = meniscus radius (m).

The *Laplace* equation may also be written as:

$$\Delta p = \frac{2\gamma}{r} \tag{4}$$

where: Δp= difference of pressure in capillaries,
γ = surface tension of water,
r = radius of water meniscus.

In Equation 3 and 4, due the similarity of two equations, we deduce that the suction is actually the change of pressure in the water held in capillaries.

The effect of pore size (radius) is also by Kelvin's equation (Janz, 2000). Water vapors condenses at lower pressure in the capillary pores than in atmosphere. The Kelvin equation gives the pore radius relation with the relative humidity of concrete. As the pore size increases, the pores may lose water relatively easily and moisture of concrete decreases, giving rise to the capillary pressure.

$$\ln \emptyset = -\frac{2\sigma M}{\rho RTr} \tag{5}$$

where: ϕ = relative humidity,
σ = surface tension of air-water interface (~0.074 N/m), and
M = molar weight of water (18 kg/Kmol),
ρ = density of water (998 kg/m^2),
R = gas constant (8.214 J/Kmol^{o}K), and
r = pore radius (m).

The Kelvin equation is also written as:

$$r = -\frac{2\gamma V}{RT \ln\left(\frac{p}{p_0}\right)} \tag{6}$$

where: γ = surface tension of water,
V = molar volume,
R = molar gas constant (8.214 J/Kmol^{o}K),
T = temperature (K),
r = pore radius (m),
p = vapor pressure (Pa),
p_o = vapor pressure of saturation (Pa)

However, combining the Laplace and the Kelvin equation allow us to see the relation between relative humidity of concrete and suction pressure, hence the induced stresses and shrinkage. The suction pressure increases with decrease in humidity. This effect has been confirmed by laboratory experiments in detail.

$$\ln \emptyset = \frac{sM}{\rho RT} \tag{7}$$

In case of excess bleed water on the surface of concrete, drying shrinkage may not occur, as there is a blanket cover of water allowing for evaporation at all times without increasing capillary pressure. Only when evaporation rate is higher than bleed water rising, drying shrinkage is observed. However, the questions regarding the validity of the *Laplace* and the *Kelvin* equation and the discontinuity of pore water in hardened paste require further elaboration with experimental results (Wittmann, et al., 2009).

2.2.5 Thermal

Temperature change may result in thermal deformation of concrete in the form of expansion or contraction. It can occur in both early and later age of concrete due to either heating or cooling. Hydration reactions release heat that cause concrete mass to expand. During the first 12 hours, the heat evolution rises and the concrete may expand due to it. This heating is often followed by a stage of cooling, which causes contraction or shrinkage of concrete. Thermal fluctuations are problematic when the rate and overall magnitude of temperature change is very high. It is also detrimental if a large temperature gradient exists over concrete's cross-section. Part of the thermal expansion is non-elastic and appears as early-age deformation. The temperature gradient is a potential cause for

cracking between layers of concrete due to differential strains and differential drying of moisture. The problem of temperature gradients is more pronounced in mass-concretes with massive cross-sections, as it takes longer for achieving thermal equilibrium.

Hydration of cement is an exothermic reaction. Therefore, the origin of heat can be traced to the cement paste. Thus, more amount of cement in a concrete mixture will result in greater amount of heat generation. However, cement alone does not govern thermal deformations. Aggregates, water-to-binder ratio (w/c), admixtures, ambient conditions and in some reported cases, fibres control the overall thermal deformations of a concrete composite. The overall hydration-based temperature effect is expressed in the form of *thermal expansion coefficient (TEC)* of concrete. Similar to hydration reactions, TEC is a dynamic property, a function of time. As explained earlier, concrete undergoes different developmental stages. There is a continuous evolution in the physical mass of concrete before it becomes hardened. Due to this, TEC is also changing very rapidly in the early stages and later it becomes more stable. Many researchers have done the estimation of TEC. The CEB/FIP model code for concrete structures has given the following expression for calculating thermal expansion [1990]:

$$\varepsilon_{cT} = \alpha_T \Delta T \tag{8}$$

where: ε_{cT}= thermal strain,
ΔT= temperature change (K),
α_T= coefficient of thermal expansion (K^{-1}).

A value of $10(10)^{-6}$ K^{-1} is used commonly for structural analysis purpose (quartzite aggregate). Furthermore, the model code states that TEC depends on aggregates type and moisture state of concrete. However, this TEC is an oversimplification of the thermal deformation phenomenon. A more nuanced approach has been adopted in this work. In addition, the time-temperature maturity concept was adopted to adjust the concrete age for more realistic estimation of TEC.

The TEC of water at 23 ^oC is $237(10)^{-6}/^oC$ (Kell, 1975). Fresh concrete at early age is more fluid; therefore, a high value of TEC is expected. The cement paste and aggregate have dissimilar TEC. The cement paste TEC varies from $11(10)^{-6}$ and $20(10)^{-6}$ per ^oC and linear TEC for air-cured concrete with gravel and limestone is $13.1(10)^{-6}$ and $7.4(10)^{-6}$ per ^oC, respectively (Neville & Brooks, 2010). The TEC for gravel and limestone concrete is with a 1:6 cement-to-aggregate ratio. The coefficient of concrete is a resultant of these TEC for the cement paste and aggregates. Greater cement-to-aggregate ratio in a mixture will result in a lower TEC. Within cement paste, TEC can be further classified as true Kinetic coefficient and swelling pressure. The swelling pressure is the effect of decreasing capillary tension of water due to the increasing temperature. During heating, moisture is transferred from the gel to capillary. Conversely, during cooling, the moisture diffusion occurs from the capillary to gel.

The moisture condition of the cement paste only contributes to the thermal deformations when the paste is partially saturated. If the paste is dry, capillaries are unable to supply water to the gel. Similarly, when the paste is saturated, there is no water menisci in the capillary. In both these extremes, the effect of a temperature change is not observed.

2.3 Mechanisms of Shrinkage Deformation

Concrete is susceptible to shrinkage and as such various have been made to explain the mechanism of the volume change in concrete. Shrinkage is the outcome, which is caused by inter-play of variety of factors. The shrinkage effects have their origin in the ingredients of concrete, the way they react together and the effects that surrounding environmental factors has on the fresh and hardened concrete. These factors can be listed as:

- Change in moisture content of concrete.
- Chemical reactions of the ingredients.
- Physical interaction of the surface of the nanoparticles of hydration products with the pore solution (Wittmann, et al., 2009).

Authors have tried to establish the link between capillary action of pore moisture with drying shrinkage (Baroghel-Bouny, et al., 1999; Hua, et al., 1995). Others explain shrinkage as the moisture content controlled disjoining pressure and surface energy as the driving force for shrinkage (Wittmann, et al., 2009; Churaev & Derjaguin, 1985; Beltzung & Wittmann, 2005). The motivation behind understanding shrinkage in early and later age of concrete is to control such harmful effects as cracking that it may cause.

Shrinkage may cause significant contribution to the risk of cracking. Even during ideal curing conditions, autogenous shrinkage may occur when there is no net moisture transfer to the environment. Investigation of the chemical and physical process in the first few hours of mixing of concrete or mortar ingredients can give answers for autogenous shrinkage. Factors such as bleeding and hardening time are very significant for autogenous shrinkage (Holt, 2000). Researchers claim that early age drying shrinkage can be eliminated by proper handling and curing practices. This may be achieved by providing time to gain strength and managing the loss of water to evaporation. Several mechanisms simultaneously or consecutively occur causing volume changes.

Syneresis is the internal reaction of bond formation/attraction between particles causing them to contract and expulse water from the pores (Brinker & Scherer, 1990). This process of phase transformation of gel material from fluid and behaving like a pseudo-elastic solid is used to explain ceramics formation. Similarly, liquid concrete phase loses water due to evaporation and contraction occurs. Evaporation drives capillary pressure, which is understood to be a cause of shrinkage from decades. An analogy between syneresis of gel material and autogenous shrinkage of concrete, where there is no moisture loss from material, can be considered as a mechanism explaining shrinkage.

2.3.1 Capillary Pressure

Radocea (1992) has explained about the origin of rise of capillary pressure form the evaporation of water from concrete. When the rate evaporation is faster than the rising bleed water, a kind of suction developed in the concrete paste due to which it contracts. Considering two cement particles at surface undergoing drying. The atmospheric pressure on the concave (upper) side is greater than the pressure on the liquid convex (lower) side. This forces the particles downward and the capillary pressure increases.

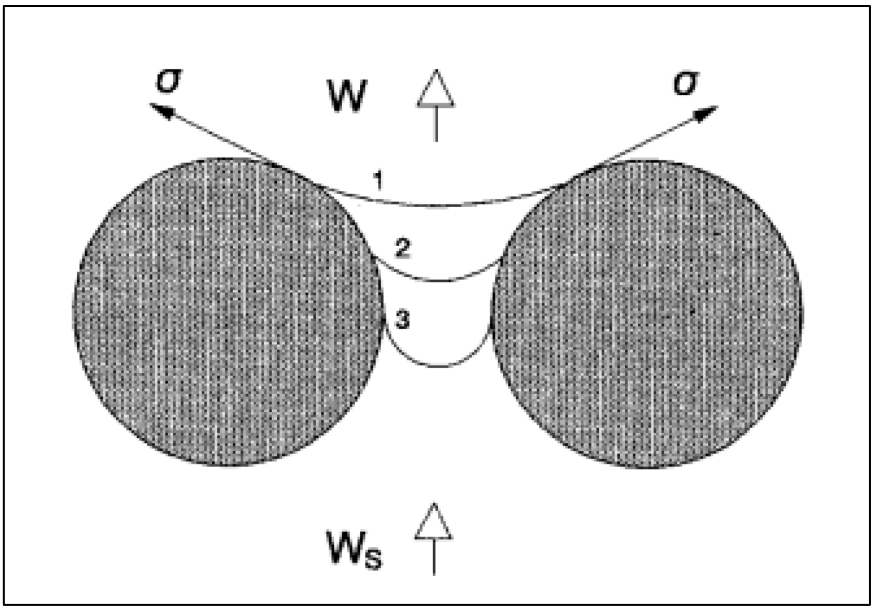

Figure 2 Water meniscus getting lower (1, 2, 3) from the pull of stresses between two cement particles as moisture transfers and capillary pressure develops. (Radocea, 1992)

Shrinkage during the plastic stage is called plastic shrinkage. Plastic shrinkage effects with highest contraction were reported within the range of w/c of 0.5 to 0.6 (Wittmann, et al., 2009). Authors of various research publications have suggested that chemical shrinkage is mistakenly considered the sole cause of plastic shrinkage stating that not much hydration occurs in the first 2 hours of mixing.

The bleed water film on top of the concrete member depends on the degree of compaction and mix proportions. The evaporating water near the surface forms a system of menisci. A pressure within the liquid phase is created due to capillary action. Gauβ-Laplace equation for the capillary pressure as presented as follows (Wittmann, 1975):

$$P_c = \sigma \left(\frac{1}{R_1} + \frac{1}{R_2}\right) \tag{9}$$

where: σ = surface tension of the liquid,
R_1 and R_2 are the main radii of the curvature of the surface of the liquid.

Particles separated by a liquid film are under action of attractive forces. For two spheres with radius R held together by a liquid ring of diameter R, the attractive force f_a is as follows (Wittmann, 1975):

$$f_a = \pi\sigma R \tag{10}$$

These small attractive forces reduce the mean distance of particles from each other in fresh concrete. Hydration results in interlocking and skeleton formation. This is why in Wittmann's explanation about shrinkage, capillary pressure is an important factor to describe plastic shrinkage (Wittmann, et al., 2009).

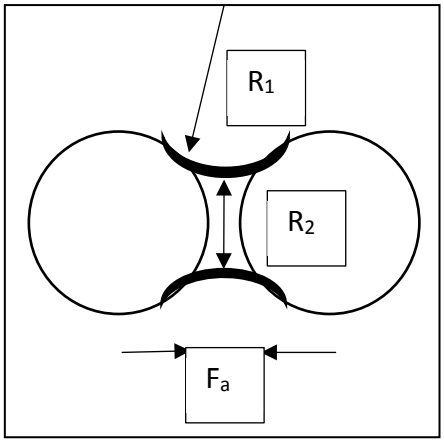

Figure 3 Liquid filled joint causing attraction between two spherical bodies.

Experimental demonstrations reveal that, when evaporation is allowed, capillary pressure builds up in pores and the rate of increase of pressure becomes large at about 2 hours after mixing. It attains a maximum value near 4 hours and then it drops further (Wittmann, 1975). The capillary water arrangement is redistributed because it becomes unstable. This maximum pressure is referred to as the *breakthrough* or *critical* pressure. Remaining water now is unable to fill all pores and voids. The complex system of menisci is thus formed. Now the capillary pressure increases in discrete zones. He also found out that plastic shrinkage measured on a linear scale is directly proportional to capillary pressure. However, the stiffening and hardening (skeleton formation) resists the contractions due to capillary pressure as hydration goes on. Considering strength development in concrete, it is possible to make simple deductions that plastic shrinkage can be reduced if:

- Critical pressure magnitude becomes less, or
- Time required to reach the critical pressure is large enough for fresh concrete to already reach some strength.

2.3.2 Disjoining Pressure

Wittmann along with Beltzung in 2009 focused on slightly different approach regarding the shrinkage mechanism in cement concrete. The *disjoining pressure* in the nanopores of hydration products of Portland cement was considered as the main cause of shrinkage. Moreover, that pore solution composition could be optimized to reduce disjoining pressure to keep shrinkage minimum (Wittmann, et al., 2009). Water penetrating into small gaps is understood to create a disjoining pressure $\prod$. Disjoining pressure arises from a complex interaction between water and two solid surfaces. It is the superposition of the repulsive and attractive forces. It can be written as follows (Wittmann, et al., 2009):

$$\prod = \prod_m + \prod_e + \prod_s \tag{11}$$

where: $\prod_m$ = molecular forces of attraction or dispersion (van der Waals forces).
$\prod_e$ = repulsive diffuse electric double layer forces.
$\prod_s$ = effects of solvation or hydration.

In hardened cement paste, the electric double layer force depends upon ion concentration and the pH value. In a vacuum, an attractive force controls interaction of solid particles. However, in a water-based solution, water penetrates the gap, and separates the surface of particles. To elaborate this further, consider the following figure 4.

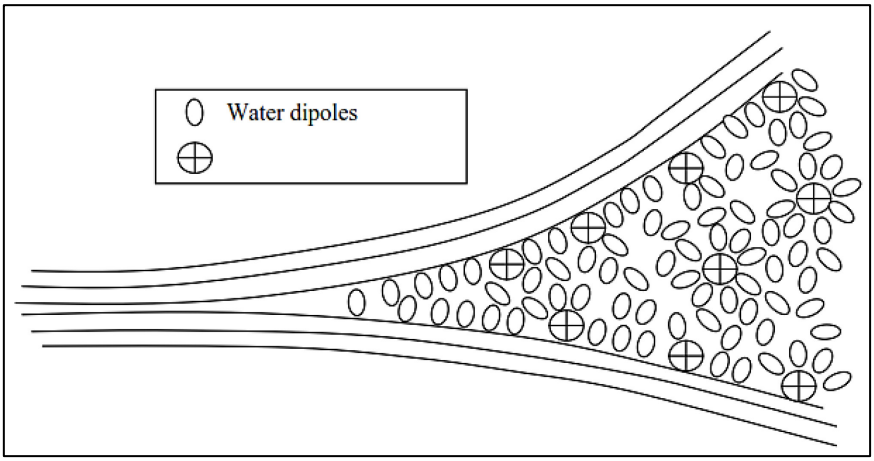

Figure 4 Nanopore model representation (Wittmann, et al., 2009).

The figure 4 shows a model nanopore filled with pore solution in CSH gel. The pore solution comprise of representative ellipses showing water molecules and positively charged ions (calcium and alkali) shown by circles with '+' sign. Negatively charged gel surface orient the water dipoles and attract some ions as in the figure. A *diffuse electric double layer* is formed near surfaces that contributes to the disjoining pressure. And *hydration shells* are formed around the ions. The zeta-potential of *diffuse layer* is less during hydration with fewer ions in pore solution. In this way, there are less gaps between cement particles during hydration, consequently less room for shrinkage. This discussion suggests that shrinkage can be modified by changing the chemical composition of the pore solution.

2.4 Fibre Reinforced Concrete (FRC)

The discussion in this section explains how fibres function in the brittle-matrix of cement concrete. The properties of fibre reinforced concrete (FRC) are still in the process of discovery but the primary function of the fibres is to mitigate cracking or reduce crack-propagation (Brandt, 2008; Holt, 2001). The classical methods applied for conventional reinforced concrete are not applicable in case of Fibre Reinforced Concrete because of random orientation of fibres (Zollo, 1996; Eik & Puttonen, 2011). Initially, fracture mechanics (FM) concept helped in the development of theories about FRC behavior. But due to lack of development of fibre production, conventional strength of materials (SOM) concept as in case of traditional concrete, were used which focus on post-cracking analysis. A large amount of energy is absorbed during the cracking process. The closely spaced fibres work to stop or slow down crack advancement by absorbing energy or transferring it to adjacent areas of less stress. FRC allows for replacing a single or two large cracks by a dense system of micro-cracking (Brandt, 2008). Concrete being a brittle material fail against tensile stresses much lower than compressive stresses because the tensile strength is approximately 7-11% of its compressive strength (Mehta & Monteiro, 2006). Fibres enhance the tensile behavior by either preventing cracking or mitigating crack-growth.

The fibres in the mixture take up the effects of internal stresses originated from shrinkage and other factors. In simple words, crack control is achieved through energy absorption via (Zollo, 1996):

- Fibre rupture,
- Fibre pullout,
- Fibre bridging and,
- Debonding at the matrix-fibre interface.

This becomes an important indicator to establish the use of fibres in reducing shrinkage-induced cracking tendency. The influence of fibres on cracking behavior is more dominant after the crack begins to open than in pre-cracking phase. In high-performance fibre-reinforced concretes (HPFRC), the tensile strength, flexural strength, and ductility performance, all are improved due to fibres addition (Shah & Weiss, 2006). Zollo (1996) reaffirms the use of fibre to inhibit cracking, control the brittle fracture process, and provide reliable post-cracking strength and toughness (Zollo, 1996).

2.4.1 Mechanics of Fibre Reinforced Concrete

Fibres add ductility to the concrete matrix with the energy absorption property making concrete less brittle. However, the efficiency of fibres depend upon fibre-matrix interactions. The interaction are divided into two parts; *friction between fibres* and *the matrix and physical/chemical bond* (Abbas & Khan, 2016). This interaction is further explained by phenomenon such as:

- Interfacial debonding,
- Plastic material deformations,
- Mechanical bond deformations and,
- Frictional sliding.

The role of fibre in concrete has been divided into *pre-cracking* and *post-cracking regime* by some authors. The mechanics of fibre-matrix interfacial bond is a complex phenomenon. The *fibre bridging-debonding-pullout* is termed as the most possible failure mode of FRC (DiFrancia, et al., 1996). The single-fibre pullout test employed by DiFrancia et al. (1996) tells about the tensile failure of fibre-reinforced composite materials. It is of interest to understand the fibre resistance against tensile forces to establish the credibility of using fibres to counter the effect of shrinkage-induced stresses. The figure shows a probable failure mode in FRC. It can be safely assumed that fibres do act to mitigate the effects of crack-inducing stresses.

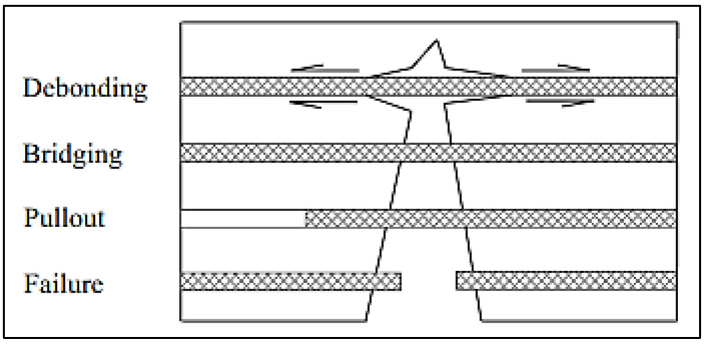

Figure 5 Fibre-matrix interactions (Abbas & Khan, 2016).

Fracture mechanics-based models help predict the development of crack under loading. In reality, load-free concrete is not possible while it is in service. The process of fracture is stated as (Jenq & Shah, 1986):

- Growth of subcritical crack,
- Beginning of fibre bridging tendency,
- Post-critical crack growth and,
- An ultimate stage when fibre remains the only resistance to crack separation.

2.4.2 Fibre Effect on Shrinkage

Fibre-matrix interaction reaffirms the efficacy of the fibres to resist cracking development. Literature review shows multiple attempts in using fibres for crack-control in concrete. Various attempts have

been made to establish usefulness of fibres in controlling volumetric changes in concrete. Apart from the properties like elastic modulus, geometry, material nature (steel, plastic, etc.), dosage, hybrid configuration (fibre type and length) of fibres are also used in FRC applications. The earliest fibres tested were coarse, 0.15 to 0.25 mm diameter, and stiff which caused mixing and placing problems (Zollo, 1996). There was hurdle of producing concrete with close enough spacing of distributed fibres with high concentration. As such, steel fibres of 50 mm length were also tested (Zollo, 1996). Longer fibres meant less number of fibres in total, i.e. greater fibre spacing.

Over the years, FRC has found applications as:

- Refractory precast concrete.
- Extruded FRC, a pressure forming technique that prevents segregation and bleeding through improved fibre-matrix bonding (Zollo, 1975).
- Fibre-reinforced cellular concrete (FRCC), which is lightweight with only voids and fibre as the aggregate phase (El-Aryan, 1995).

FRC has been studied and used in the academia and industry for decades now. Over the years, authors have tried to list down benefits and shortcomings of FRC. Despite rich and large knowledge of FRC, the practical application are not numerous. Dispersed fibres are used to control the crack opening and propagation but this use is not an exact science. Different type of fibres have been grouped as (Brandt, 2008):

- Steel fibres (different shapes and dimensions),
- Glass fibres (e.g. alkali-resistant fibres),
- Synthetic fibres (e.g. polypropylene, polyethylene, polyolefin, polyvinyl alcohol),
- Carbon and pitch fibres and,
- Poly-acrylonitrile (PAN) fibres.

Asbestos fibres are no longer used due to health hazard. Higher fibre volumes are known to reduce workability and make the concrete weaker as they displace aggregates form their place during mixing and may create ITZs. However, the use of admixtures with reduced w/c as in case for high-strength concrete is a solution for workability related issues. Fine fibres control opening and propagation of micro-cracks as they are densely dispersed. The high performance commercial concretes like Ductal® and BSI® use hybrid fibre reinforcement of different size of steel fibres, which control micro-cracks and also eliminate the use of passive steel reinforcement. A brief summary of research in the use of fibres for crack control is shown in Table 1.

Table 1 Summary of previous research in the use of fibres for crack control.

Authors	Year of Publication	Contribution
Swamy et al. (Swamy & Stavrides, 1979)	1979	The shrinkage of a 1.0% by volume of steel or polypropylene fibres composite is 20% less than that of a comparable plain concrete.
Zollo , Zollo et al. (Zollo, 1984; Zollo, et al., 1986)	1984, 1986	The drying shrinkage of concrete maybe reduced up to 75% using appropriate quantity of polypropylene fibres.
Chuan et al. (Chuan & Young, 1990)	1990	It was reported that the aspect ratio of fibres also has influence on the reduction of shrinkage. Also, shrinkage of composite containing longer steel fibres in less than that of similar composite containing short fibres.
Paillere et al. (Paillere, et al., 1989)	1990	The autogenous shrinkage of a composite with 0.8% by volume of fibres is less than that of a comparable HPC.

Kovler et al. (Kovler, et al., 1992)	1992	The crack width is reduced to approx. 50% using polypropylene fibres. The plastic shrinkage is reduced as well.
Kovler et al. (Kovler & Bentur, 1997)	1997	The addition of steel fibres do not cause any reduction in composite shrinkage.
Balaguru et al. (Balaguru & Ramakrishnan, 1988)	1988	The shrinkage results after 500 days of a composite with 55 MPa compressive strength was 10% less than that of a comparable concrete without fibres.
Barr et al. (Barr & El-Baden, 2003)	2003	The optimum fibre content for reduction of composite shrinkage is 1.0% by volume. Any amount of fibres greater than this did not show a significant further reduction of shrinkage.
Kamen (Kamen, 2006)	2006	The autogenous shrinkage of an ultra-high performance composite (UHPC) with 6.0% by volume of steel fibres was 35% less than that of a comparable concrete without fibres.
Banthia et al. (Banthia & Gupta, 2006)	2006	Thinner and longer polypropylene fibres are more effective in reducing early plastic shrinkage than thicker and shorter ones.
Sandbakk (Sandbakk, 2007)	2007	The optimum fibre length is somewhat larger than the maximum aggregate size. Non-metallic fibres has considerable reducing effect on the early-age shrinkage and are better than steel fibres to prevent plastic shrinkage. However, adding steel fibre on top of the maximum content of non-metallic fibre may give the best result.
Myers et al. (Myers, et al., 2008)	2008	The polypropylene fibres in FRC have a small effect in reducing the composite shrinkage.
Aly et al. (Aly, et al., 2008)	2008	Observed 15% greater shrinkage with use of 0.50% by volume of polypropylene fibres (RH of 50%, 23^{o}C, 1 day curing). And for 7 days of curing with same RH and temperature, 22% greater shrinkage was observed. However, these results could be the effect of accelerated evaporation conditions.
Saje et al. (Saje, et al., 2012)	2012	Steel fibres are more effective than dry polypropylene fibres for reducing early shrinkage. However, the polypropylene fibres are equally effective as steel fibers in reduction of later autogenous shrinkage. Least amount of total shrinkage occurred using polypropylene fibres. 17% to 29% less shrinkage was observed than that of comparable plain concrete. Short steel fibers are more effective in 0.75% by volume concentration. However, in case of 0.25% and 0.50% by volume of steel fibres, longer fibres are more effective.
Kaikea et al. (Kaikea, et al., 2014)	2014	In 10% silica fume, using 1% by volume of corrugated steel fibres resulted in 28-day shrinkage reduction of 4% to 9% compared to plain concrete. In 20% slag, using 2% by volume of steel fibres resulted in 15% to 24% shrinkage reduction at 28 days.
Mangat & Azari (Mangat & Azari, 1984)	1984	Increased amount of steel fibre volume has greater reduction of drying shrinkage.
Bywalski et al. (Bywalski, et al., 2015)	2015	Using 3% by volume of straight steel fibres reduces 28-day total shrinkage by 32% compared to plain concrete.

Chen & Chung (Chen & Chung, 1996)	1996	Using 0.19% by volume short carbon fibre with 15% silica fumes resulted in 84% reduction in the drying shrinkage strain of concrete compared to plain concrete.
Sivakumar et al. (Sivakumar & Santhanam, 2007), Choi et al. (Choi, et al., 2011)		The drying shrinkage is reduced by the addition of polypropylene, PVA, polyester, glass, nylon and, cellulose fibres in the concrete.
Sun et al. (Sun, et al., 2001)	2001	Hybrid steel fibres reinforced concrete have lower shrinkage strain than concrete with large sized fibres. Hybrid steel fibres caused 10%-34% and 45%-65% reduction in 28-day shrinkage strain of the concrete compared to the specimen with 1.5% large steel fibres and plain concrete.

2.4.3 Brief Summary of Fibre Use in Concrete

FRC has many more applications in affecting the non-structural serviceability aspects of the design of concrete. Fibres improves the serviceability through durability and toughness by controlling cracking. The idea of crack control is for aesthetic and serviceability-related aspects through reducing the crack width and area (Zollo, 1996). The applications with low fibre content of fibres reduce the workability problems. Low fibre volume applications (<0.5% by volume of fibre) include slab-on-grade and composite deck.

The use of 0.1% - 0.5% by volume steel and synthetic fibre is for crack control rather than increasing load-transfer capacity (Padron & Zollo, 1990). Afroughsabet et al. (2016) concluded after a study of 370 review papers that fibres have a mixed effect on the shrinkage and cracking of concrete (Afroughsabet, et al., 2016). The work of researchers in studying the effect of fibres on the drying shrinkage of concrete have returned contradictory conclusions sometimes. Some studies showed that fibres had an insignificant effect on the shrinkage. Others showed a real contribution of fibres in reducing the shrinkage of FRC.

The effectiveness of fibers in reducing shrinkage and cracking is dependent on the elastic modulus of fibers in addition to their size and content (Afroughsabet, et al., 2016). From the literature review, it was observed that:

- Increasing the amount of fibres was not always helpful to reduce the shrinkage.
- Short fibres in great resulted in a larger decrease in the shrinkage compared to the use of longer fibers.
- The greater dispersion helped in transferring the stresses in the matrix.
- Introducing non-metallic fibers and particularly nylon fibers was very helpful in reducing the shrinkage of concrete.
- The hybrid mix of steel fibers of different sizes or combining with nonmetallic fibers also reduced the drying shrinkage of concrete.
- Sandbanks (2007) proposed the use of saturated cellulose fibres to provide internal curing to mitigate shrinkage cracking in hardening phase (Sandbakk, 2007).
- In general, literature shows that steel fibres are less effective than non-metallic fibres. The logical reason could be the number of fibres (dispersion). As non-metallic fibres are thinner, thus in a certain volume non-metallic fibres pack greater number of fibres than metallic fibres of same volume.

However, considering the addition of fibres as a one-key solution for crack control may be an oversimplification of a complex process of concrete shrinkage. Rather, while maintaining suitable

ambient conditions (temperature, wind and RH) and mix proportions, a particular type of mixture may take the effect of fibres in successful crack control.

2.5 Challenges of Concrete Shrinkage

Based on above discussions, the total shrinkage in the cement paste or concrete can be considered as the sum of following:

- Autogenous deformations.
- Drying shrinkage.
- Thermal deformation.
- Due to carbonation.

The explanation of shrinkage via disjoining pressure is different from other capillary pressure and syneresis approaches. The disjoining pressure approach explains the inherent shrinkage potential of the cement concrete. This potential depends upon the interaction of pore solution with the hydration products. If the zeta-potential is small, the hydration products are closer to each other and pores are of smaller size, there is less room available for contraction upon drying.

Design codes are guilty of using ultimate shrinkage effects corresponding to long-term drying shrinkage usually. However, like in the case where evaporation rate is less than bleed water rising or evaporation is totally avoided, autogenous shrinkage effects can be equal or more than the long-term effects. In addition, autogenous shrinkage has a major share in case of low w/c ratios like in case of high strength concretes.

In slabs or floors, where the concrete is exposed, curing water or re-absorption of bleeding water can ensure complete hydration and minimizing autogenous shrinkage effects. However, in situations when curing water is not available and concrete is of low w/c ratio, all drying shrinkage is result of autogenous, internal effects. Plastic shrinkage is usually known for detrimental effects in the concrete slabs. However, if serious cracking can be avoided, plastic shrinkage has a compacting effect leading to improved mechanical behavior (Wittmann, 1975).

The Kelvin and Laplace relations help explain the shrinkage causes in a mathematical way. Cement paste or concrete particles are brought closer as the capillary pressure forces the water meniscus between the pores. The shrinkage stresses are found to be dependent on the following factors:

- Porosity of the cement paste or concrete (density).
- Ingredients of the mixture as they influence the pore sizes (for example; silica fumes).
- Mix proportion parameters (for example; w/c ratio).

There seem to be more than one explanation for the shrinkage in concrete. All the processes involved and phenomenological approaches are equally difficult to deny or accept. One thing is certain, that shrinkage effects are associated with cement-based mixtures owing to the hydration process involved. The technique to control shrinkage effects could be multi-pronged assuming the causes are also manifold.

2.6 Test Procedures

2.6.1 Early Age Autogenous Shrinkage

The inherent difficulties of test arrangements present a challenge to accurately measure early age shrinkage of concrete in laboratories. Nowadays, test setups are available which allow measurements of linear and volumetric shrinkage from minutes after the mixing of water and cement. Various test setups are available due to fast-paced improvements of technology. This makes measurement of the early age shrinkage a challenge due to influence of each test procedure.

Test Setup: Roziere et al. have presented the comparison of results of early autogenous shrinkage measured from using four different test setups (Roziere, et al., 2015). It was concluded that all test methods showed significant differences of the shrinkage magnitudes, proving the influence of test procedure on measurements. A general guideline for test setup for measuring autogenous deformation is as follows (Roziere, et al., 2015; Bjontegaard & Hammer, 2006):

a) Specimens to be totally sealed to prevent any moisture exchange.
b) Limited friction between the specimen and mold.
c) Test setup equipped with automatic data logging.
d) The maximum temperature increase in concrete not greater than 2 ^{o}C.

In case of absence of any temperature control with the test setup, autogenous deformations are uncoupled from thermal deformations (Section 2.2.5). It is important that the adopted test method show repeatability and consistency in the results both qualitatively and quantitatively. For later comparison, it is very important that the test be conducted in the same unchanging laboratory environment for results credibility. Linear measurement is a reliable parameter to quantify autogenous shrinkage (Roziere, et al., 2015). Configuration of the test rigs, horizontal or vertical, also affects the measured autogenous shrinkage. Moreover, a choice of moulds (flexible or rigid) is another parameter that affects autogenous shrinkage measurement.

Test methods are of two broad categories: *volumetric* and *linear* measurements (Roziere, et al., 2015). Cement pastes and mortars are subjected to volumetric methods whereas; linear measurements are made with concrete specimens. Rigid moulds may underestimate the magnitude of autogenous shrinkage due to friction effects between the mould and the specimen (Barcelo, et al., 1999). This friction may be minimized using a membrane between sample and frame. Roziere et al. (2015) suggest the use of plastic foil with talcum powder to reduce friction.

Different time-zero (time when measures are initialized) may give different and compromised results for shrinkage (G, et al., 2006). To differentiate from the chemical shrinkage, the setting time is often chosen for time-zero (Roziere, et al., 2015). The selection of time-zero is complicated as there are different ways of assessing setting of concrete, which results in different time-zero values (Tazawa, et al., 2000). Eppers and Mueller (2008) suggests time-zero through minimum of the shrinkage rate as this time corresponds to the time when stresses are generated in ring tests in restrained (Eppers & Mueller, 2008).

Despite receiving plenty of research focus, early age shrinkage measurements still need across the board standardizing. Kucharczykova et al. have demonstrated a method of measuring early age linear shrinkage of cement composite (Kucharczykova, et al., 2017). The experiment was performed with equipment standardized according to the Austrian standard OENORM B 3329:2009-06-01. The test mold was 1000 mm in length, and with a 60 x 100 mm cross-section. Length changes are recorded along the central axis of the specimen with a sensor resting against movable head of mold, which is partially cast into the fresh sample. The other end of the sample is restrained with transverse screw running through the sample. A polyethylene foam of 2 mm thickness was placed inside the mold to minimize friction and allow the sample to deform because of shrinkage. The apparatus is placed on a weighing scale table to measure the mass loss. The test setup allowed for recording of specimen temperature with the help of a thermocouple. The test setup was found to be an implementation of the guidelines explained by Bjontegaard and Hammer (2006) and Rozieri et al. (2015) for linear early age shrinkage test setups. The molds can be encapsulated by providing lids or covering the fresh samples completely with polyethylene sheet to setup autogenous test conditions.

For this research work, Schleibinger Bending-Drain was used for the measurements of early age autogenous shrinkage. The test equipment is pursuant to a draft European Standard prEN–13892–

9:2017(E). More details about the procedure of early-age autogenous shrinkage rig test and data analysis is given in Section 4.3 and Section 5.1, respectively. Autogenous conditions were maintained by wrapping the sample completely with polyethylene sheet of 2 mm thickness.

2.6.2 Long-term Free Drying Shrinkage

Long-term shrinkage of concrete is usually measured by laboratory tests with prismatic concrete members. ASTM C157 is one such common example of a 'standard test method for length change of hardened hydraulic-cement mortar and concrete'. The principle is to measure the length changes due to factors other than externally applied forces and temperature changes in hardened mixtures (concrete for this work). The concrete specimens are prepared in the laboratory and cured in a defined way. The test method is useful comparative evaluation of long-term drying potential when different concretes are subjected to same curing conditions. According to this standard, a concrete specimen of length 285 mm and cross-section of 100 x 100 mm is placed in the climate room to dry. The use of length comparator and weigh scale to record successive shrinkage measurements and moisture loss is quite common to standards of different countries.

The international standard ISO 1920–8 'determination of drying shrinkage of concrete for samples prepared in the field or in the laboratory'. The principle according to this standard is again determining the length changes of concrete specimens due to drying in air. The concrete sample can have aggregate of maximum nominal size not greater than 25 mm. The samples were cured in a climate room, which maintained a relative humidity (RH) of 65% and temperature of 20 ^{o}C.

Finnish standard SFS–EN 12617–4 'products and systems for the protection and repair of concrete structures –Test methods–part 4: determination of shrinkage and expansion' specifies a method for measuring the dimensional stability (shrinkage and swelling) due to change of moisture amount in concretes. It provides two methods for measuring linear drying shrinkage, restrained or unrestrained movements. Concretes with a maximum aggregate size of 10 mm can be tested following this standard. Unrestrained linear movement from drying in air or expansion in water can be measured for prismatic specimens of length 160 mm and cross-section 40 x 40 mm.

Practices from Finnish standard SFS–EN–12617–4(2002) and International standard ISO–1920–8:2009(E) were adopted for this work. Concrete specimens with maximum aggregate size of 16 mm were cured in a climate room (20 ^{o}C and 65% RH). Wet curing was done for any specimen. Details of the procedure and methodology has been included in Section 4.4. Measurement readings of both length shortening and mass loss were taken on a pre-determined schedule of 1, 3, 7, 14, 28 and 56 days after demolding.

3. Materials

The materials used in the experimental program were mostly Finnish. The particular details are presented in the following sections. Clean tap water was used for making all the mixtures from the same source. The temperature of water was approximately 20 ^{o}C.

3.1 Cement Types

The tests in this research study were performed using three types of cement manufactured by Finnsementti Oy. The choice was based on keeping in mind various applications of different cement types and for purpose of comparison. The autogenous and drying shrinkage tests were both performed using all three types of cement. This allowed for a comparison of shrinkage magnitudes and early age concrete behavior due to different cement's chemical composition. All three cements conformed to the standard SFS-EN 197-1: 2011.

- Plus cement is a very common hydraulic cement in Finland used at a large scale in construction industry. It is classified as 'CEM II/B-M (S-LL) 42.5 N', a Portland-composite cement type with 65-79% clinker. The cement is ground to a relatively higher fineness (Blaine fineness value). The Plus cement has 21-35% inert material added as blast furnace slag (15-25%) and limestone (6-15%). The cement is of ordinary early strength class.
- SR cement (Sulfate resisting) is classified as 'CEM I 42.5 N – SR3', a Portland cement type with =>95% clinker and small percentage of limestone as inert constituent. The chemical composition of the clinker is slightly different resulting into a slightly higher 7 days and 28 days strength than Plus cement.
- White cement is the third type of cement used this work, classified has 'CEM I 52.5 R- SR5'. This cement type was selected with aim of understanding the shrinkage properties to develop the use in façade works. The clinker for white cement has greater CaO than other two cement types. It has early initial setting time compared with the Plus and SR cements and belongs to a. With negligible amount of inert constituents, the white cement has even higher 7 day and 28 day strength than Plus and SR cement. The typical properties of the three cement types and their respective clinker is given in the table 2 and 3 below.

Table 2 Finnsementti cement clinker composition (Finnsementti Oy, 2016).

Clinker Compounds	Plus cement	SR cement	White cement
CaO	63-65 %	64-66 %	69 %
SiO_2	20-22 %	20-22 %	24 %
Al_2O_3	4.0-5.4 %	3.1-3.7 %	2.1 %
Fe_2O_3	2.8-3.3 %	3.9-4.2 %	0.3 %
MgO	2.5-3.2 %	2.7-3.5 %	0.7 %
C3A	-	<= 3.0 %	<= 5

Table 3 Finnsementti cement properties (Finnsementti Oy, 2016).

Properties	Plus	SR	White
Fineness (Blaine) (m^2/kg)	420-470	380-410	390-420
28 day strength (MPa)	46-52	54-59	66-76
Initial Setting time (min)	150-210	160-200	110-160

3.2 Admixtures

Chemical admixtures were added to improve concrete characteristics like workability and air content.

- A superplasticizer (SP) called 'MasterGlenium SKY 600', made by BASF Group of Finland, was used with all three cement types to achieve the desired workability for each mixture. It is a poly-carboxyl ether based SP used in dosage of 0.2 - 2 % of binder volume and has a density of 1.03 g/cm^3 (MasterGlenium reference).
- A shrinkage-reducing admixture (SRA) was also used with Plus cement in one of the mixtures for both autogenous and drying shrinkage test. The SRA was 'MasterLife SRA 815' made by BASF Group of Finland. It has a density of 0.94 – 0.96 g/cm^3 and is used in a dosage of 0.5 - 3 % of binder volume. It works by reducing the surface tension of pore water, consequently reducing drying shrinkage (Masterlife SRA reference). The effect of SRA is more pronounced in concrete with relative humidity (RH) greater than 40% as shrinkage is surface tension controlled in this case. In pores of size 10 to 50 nm, loss of moisture causes curved menisci to pull the pore walls through surface tension. SRA relieves this inward pull and reduces the potential for shrinkage.
- In addition, an air-entraining admixture (AEA) called 'MasterAir 100', also made by BASF Group of Finland, was used with white cement. It was used as 0.042 % by weight of cement and has a specific gravity of 1.022. Small, closely spaced and stable air bubbles were introduced by using this AEA (MasterAir reference).

For most cases (Plus and SR cement concrete), the target slump was of S3 class (approximately 150 mm). Whereas, it was S4 class (approximately 200mm) for white cement concrete. The design air content for Plus and SR cement concrete was 3%, whereas 5% for white cement concrete.

3.3 Fibres

For the experimental verification of the hypothesis that fibres affect the volumetric deformations in concrete, three type of fibres were used for test. Steel, polypropylene (plastic) and glass fibres were tested by dozing an amount of 0.38% by volume of fibres concrete. However, glass fibre was added to white cement concrete only. Table 4 and 5 contain the summary of the of the respective fiber properties.

Table 4 Properties of Hooked-end (HE) Steel fibres (ArcelorMittal, 2010).

Name	Length (mm)	Diameter (mm)	Aspect ratio	Tensile strength (MPa)	No. of fibres /kg	Fibre class (EN 14889-1)
HE 1/50	50	1.0 (± 0.04)	50	1150	3100	Type 1 (cold-drawn wire)

Table 5 Properties of Plastic and Glass fibres (BASF, 2016; Owens Corning, 2015).

Name	Type	Length (mm)	Diameter (mm)	Aspect ratio	Tensile strength (MPa)	Density (g/cm^3)	No. of fibres /kg
Masterfiber 246	Polypropylene	40	0.75	53	400-450	~1.0	~65000
Anti-crack HP24	Glass	24	16µm	55	1000-1700	~2.68	-

The steel hooked-end fibre work by providing a strong mechanical resistance to crack opening inside the concrete matrix. The high tensile strength ensures increased structural performance in flexure state. The glass fibres are termed as high performance adding flexure, toughness, impact and fatigue resistance. Due to higher density, they mix very uniformly and easily throughout the concrete mixture and are claimed to control thermal, plastic and drying shrinkage by the manufacturer (anti-CRAK). These glass fibres can be both as primary and secondary reinforcement. The plastic fibres used in this work are extruded fibres with a crimpled (zig-zag) profile. The crimpled shape increase pull-out resistance and increase ductility and toughness. The mixing time is suggested approximately 5 minutes to ensure a homogeneous mix for these fibres. The fibres were added into the mixture after mixing all other ingredients. These selection fibres offered a wide range of properties; steel fibre with high tensile strength and density, plastic-polypropylene fibres with lower density and tensile strength but greater number of fibres in the same volume (see Table 4 and Table 5); fibrillated glass fibres with high strength and dispersion due to density similar to concrete.

Figure 6 A) Plastic (polypropylene) fibres. (BASF, 2016) B) Glass fibres. (Owens Corning, 2015) C) Steel fibres. (ArcelorMittal, 2010).

3.4 Aggregates

Two types of aggregates were used in the experimental program, naturally graded granitic and limestone aggregate. Finnish natural granite with a dry density of 2670 kg/m^3 with sand as the fine aggregate and rounded coarse aggregate particles. The absorption was reported to be 0.8 %. For Plus and SR cement concrete, one gradation was used with 16 mm maximum aggregate size. Table 6 shows the graphic description of the aggregate distribution.

Table 6 Aggregate gradation for Finnish natural granite for Plus and SR cement concrete.

Size (mm)	Passing (%)
0.125	3.7
0.25	8.7
0.5	15.2
1	24.2
2	38
4	48.5
8	67.5
16	99.6

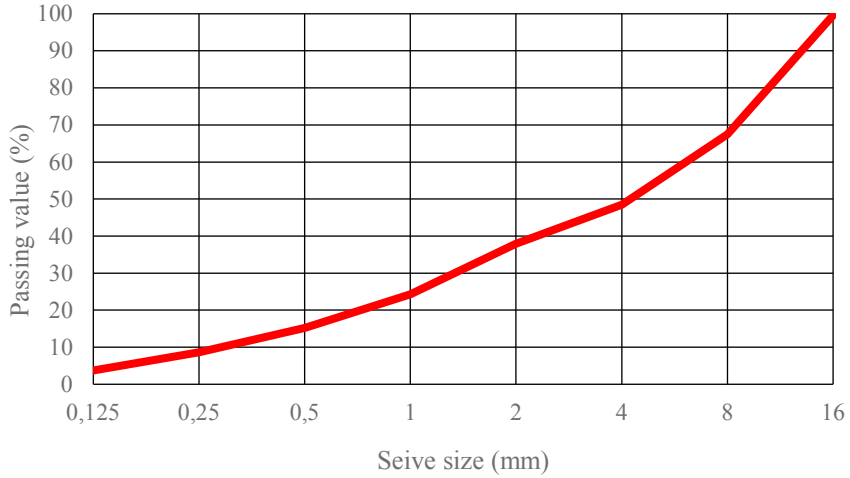

Figure 7 Gradation curve of Finnish natural granite aggregate.

White-gray Limestone aggregate (22R) of Finnsementti Oy was used for white cement concrete. Unlike Finnish natural granite, four aggregate fractions were used including both fine and coarse aggregate. 22R is a metamorphic rock of calcium with a dry density of 2.75 kg/m^3. The absorption was reported to be 0.8 % and was as such accounted for in the mixture design. The maximum aggregate size of 12mm was used. A high amount of limestone filler (20%) was used in the white concrete recipe. Following table 7 shows the fraction portion of the limestone 22R aggregate.

Table 7 Finnsementti Limestone 22R aggregate portions.

Size (mm)	Fraction portion (%)
Filler TY	20
0 – 2	40
2 – 5	20
4 – 12	20

3.5 Mixture Design

As mentioned in previous section, three generic concrete mixtures were prepared based on three cement types. The mix design of concretes for Plus and SR cement same, using same aggregate type and gradation, amount of SP, cement and water/cement ratio. However, separate design was used for white cement concrete. Moreover, same mixture design were used for the test of drying and autogenous shrinkage. The required amount of SP and AEA for target slump and air were decided by trial batches before actual test series. Table 8 presents the mixture proportions for Plus and SR cement concrete, whereas Table 9 presents the mixture design for white cement concrete.

Table 8 Mixture design for Plus and SR cement concretes (autogenous deformation and drying shrinkage test).

Cement (kg/m^3)	385
Water (kg/m^3)	194
Aggregate (kg/m^3) Natural Filler	 143 (8%)
R 0.1/0.6	161 (9%)
R 0.5/1.5	161 (9%)
R 1.0/2.0	268 (15%)
R 2.0/5.0	268 (15%)
R 5.0/10.0	214 (12%)
R 8.0/16.0	572 (32%)
ALL (kg/m^3)	1787 (100%)
Superplasticizer (% cement weight)	0.37
Air Content (%)	2.0

Table 9 Mixture design for White concrete (autogenous deformation and drying shrinkage test).

Cement (kg/m^3)	350
Water (kg/m^3)	194
Aggregate (kg/m^3) (TY 63) Limestone Filler	 353 (20%)
R 0/2	705 (40%)
R 2/5	353 (20%)
R 4/12	353 (20%)
ALL (kg/m^3)	1764 (100%)
SP (% cement weight)	1.1
AEA (% cement weight)	0.05
Air Content (%)	5.0

4 Test Procedures

Both early age autogenous and drying shrinkage were measured in this research study. The early age shrinkage was measured using Schleibinger Bending-Drain rig, which is a meter long U-shaped stainless steel mold open from the top. For simplicity, the Bending-Drain will be referred to as 'shrinkage rig' in this document. Details about the shrinkage rig are provided in the following sub-sections. For drying shrinkage test, 500 mm long beams (cross-section 100x100 mm) were cast.

4.1 Mixing

Aggregates and cement was dry weighed in the mixer prior to the addition of water. 30 liter and 40 liter batches were prepared for early age autogenous shrinkage and drying shrinkage test respectively. The mixing was done in Pemat mixer as shown in the Figure 8. It has filling capacity of either 108 liter or 120 kg with a frequency of 50 revolutions per minute (rpm).

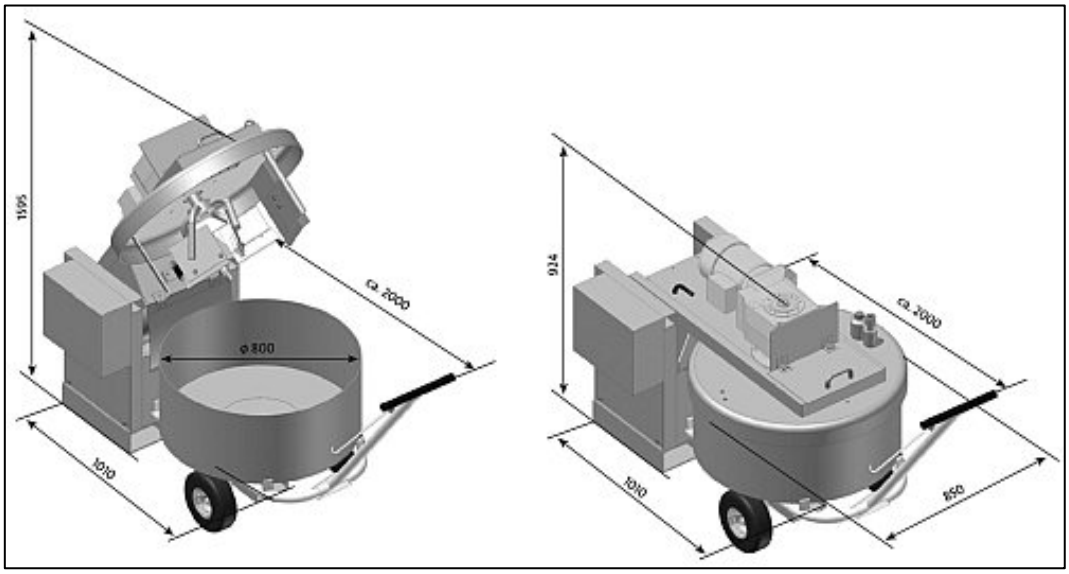

Figure 8 Pemat mixer (Pemat, 1985).

Figure 9 Pemat mixer in concrete lab, Aalto University.

Following the dry mixing of the ingredients for 30 seconds, water was added and mixing was continued for 30 seconds more. Each admixture was added with 10 % water and mixed for 30 seconds each. In the end, fibres were added to the mix at a moderate rate to avoid clusters and fibre-balls formations. The fibres were mixed for 3 minutes to get a homogenous mix in order to ensure uniform composition throughout the sample.

Beam specimens were prepared for drying shrinkage measurement. The test was carried out according to Finnish standard SFS–EN–12617–4(2002) and International standard ISO–1920–8:2009(E). To start recording shrinkage and mass variation measurements from the day of demolding, wet curing was not done. The shrinkage rig test was performed according to a draft European Standard prEN–13892–9:2017(E). Fresh concrete tests for slump and air content were also performed for the mixtures in accordance with EN–12350:2009. A summary for the standard is presented in Appendix 1.

4.2 Test Mixtures

The tests were done using three types of cement, two types of aggregates, three types of fibres and three types of admixtures. Using different combinations of ingredients, ten mixtures were prepared for both shrinkage rig and drying shrinkage test. The motivation behind this test series is to observe and measure the effects of different cements, fibres and SRA. Following mixtures, coded from one to ten, were tested in this work.

1) Plus cement concrete mixtures:
    i) M1 (Plain Concrete).
    ii) M2 (Concrete with Steel fibres).
    iii) M3 (Concrete with Plastic fibres).
    iv) M4 (Concrete with Steel fibres and SRA).
2) White cement concrete mixtures:
    i) M5 (Plain Concrete).
    ii) M6 (Concrete with Plastic fibres).
    iii) M7 (Concrete with Glass fibres).
3) SR cement concrete mixtures:
    i) M8 (Plain Concrete).
    ii) M9 (Concrete with Steel fibres).
    iii) M10 (Concrete with Plastic fibres).

A summary of composition of the test mixtures is given in Table 10 below.

Table 10 Mix proportions and properties of concrete mixtures.

Mixture Code	M1	M2	M3	M4	M5	M6	M7	M8	M9	M10
Plus Cement	✓	✓	✓	✓	-	-	-	-	-	-
White Cement	-	-	-	-	✓	✓	✓	-	-	-
SR Cement		-	-	-	-	-	-	✓	✓	✓
Cement (kg/m^3)	385	385	385	385	350	350	350	385	385	385
Water (kg/m^3)	194	194	194	194	194	194	194	194	194	194
Aggregate (kg/m^3)										
Filler TY 63					353	353	353			
Limestone 22R 0/2					705	705	705			
Limestone 22R 2/5					353	353	353			
Limestone 22R4/12					353	353	353			
Filler 96	143	143	143	143				143	143	143
R 0.1 - 0.6	161	161	161	161				161	161	161
R 0.5 – 1.2	161	161	161	161				161	161	161
R 1.0 – 2.0	268	268	268	268				268	268	268
R 2.0 – 5.0	268	268	268	268				268	268	268
R 5.0 – 10.0	214	214	214	214				214	214	214
R 8.0 – 16.0	572	572	572	572				572	572	572
Steel fibres	-	✓	-	✓	-	-	-	-	✓	-
Plastic fibres	-	-	✓	-	-	✓	-	-	-	✓
Glass fibres	-	-	-	-	-	-	✓	-	-	-
Volume of fibres % (kg/m^3)	-	0.38	0.38	0.38	-	0.38	0.38	-	0.38	0.38
SP (% by weight of the binder)	0.37	0.37	0.37	0.37	1.1	1.1	1.1	0.37	0.37	0.37
AEA (% by weight of the binder)	-	-	-	-	0.042	0.042	0.042	-	-	-
SRA (% by weight of the binder)	-	-	-	1.0	-	-	-	-	-	-
Air (dm^3/m^3)	20	20	20	20	50	50	50	20	20	20
Density (kg/m^3)	2367	2367	2367	2367	2311	2311	2311	2367	2367	2367
Slump (mm)	S3	S3	S3	S3	S4	S4	S4	S3	S3	S3

Target air for Plus and SR cement concrete mixtures was 2%, common for most mixtures. Therefore, no AEA was added for them. However, 0.042% (of binder weight) AEA was added to white cement concrete to achieve a target air of 5%. This dosage was arrived at by trial batches. Similarly, SP dosage of 0.37% and 1.10% for Plus/SR and White cement concrete mixtures was a result of trial and error for S3 class slump. The slump varied between 135 mm to 160 mm and approximately 200mm for Plus/SR and White cement concrete mixtures, respectively. Compaction for drying shrinkage beams was achieved by using vibrating table.

4.3 Early Age Autogenous Deformation Test Arrangement (Schleibinger Bending-Drain)

The early age autogenous shrinkage test was performed using Schleibinger Bending-Drain apparatus. The shrinkage rig was modified using thin polythene sheet to provide near-perfect autogenous condition. The working of this setup is explained in the standard EN–13892–9:2017(E). It is a beam apparatus, which allows for the continuous measurements of vertical and horizontal deformations, specimen & mold temperature and room temperature & humidity since the moment fresh concrete sample is placed in the U-shaped mold of the test rig. Figure 10 is a picture of the Schleibinger Bending-Drain apparatus and Figure 11 shows an ongoing test.

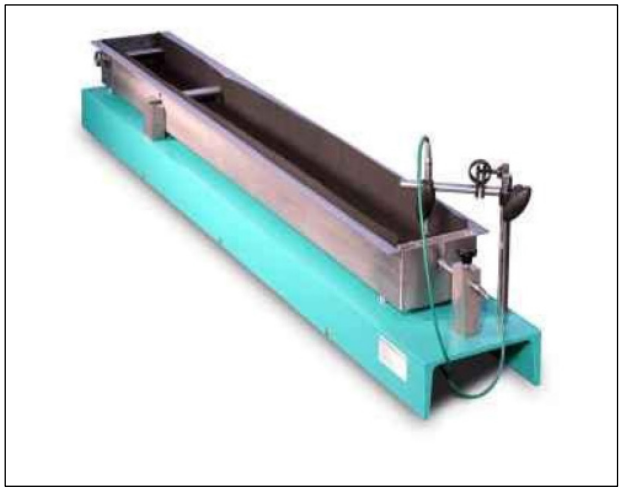

Figure 10 Schleibinger Bending-Drain (Schleibinger Geräte, 2015).

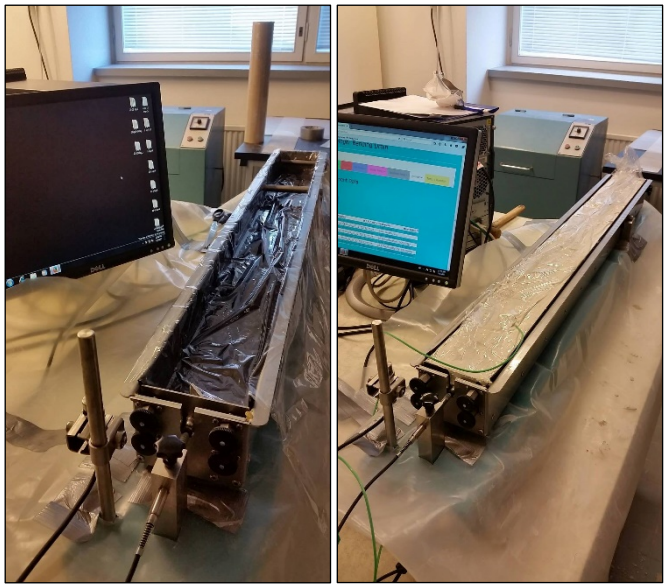

Figure 11 Picture of Early Age Autogenous Deformation Test with the Schleibinger Bending-Drain.

4.3.1 U-Shaped Stainless Steel Apparatus

The U-shaped stainless steel mold is covered with thin neoprene rubber sheet and polythene sheet to minimize mold-sample friction. The mold dimensions are 1000 x 100 x 50 mm^3 (length * width * height). Both the shrinkage and curling test can be performed for concretes/mortars. However, only

horizontal shrinkage was measured in this work. Data is continuously stored in an integrated data logger that is connected to a computer to initiate and control the test. The linear changes in specimen dimensions due to shrinkage/swelling are recorded with the help of two high resolution LVDTs (Linear Variable Differential Transformer). Two RTDs (Resistance Temperature Detector) measure the temperature development at the base of the sample (formwork) and in the specimen. Additionally, a moisture/temperature sensor also measures humidity and humidity-temperature of the test surroundings.

Table 11 Technical Data sheet – Schleibinger Bending-drain.

Name	
Measurement range in both directions	5 mm
Specimen length	1000 x 100 x 50 mm
Resolution	0.3 µm
Accuracy	± 4 µm
Maximum Temperature	70 °C
Heating	120 W @ 20 °C
Weight	36 kg

4.3.2 Test Operation

The test was started approximately 40 minutes after water is mixed with dry materials. During this time, fresh concrete properties like slump and air were measured. The concrete sample was poured into the U-shaped steel mold in two layers, which is kept in a climate room at fixed 20°C. Each layer was compacted with gentle blows of a wooden tamping rod, such as the one used for Flow table test (EN–12350–5:2009). The sample is fixed in the mold with two bolts running traverse in to the concrete specimen on one side. A movable stamp (end-plate anchor) with a hook, placed on the other side inside the mold, moves with minimum friction as grease is applied to its edges. This hook is cast into the concrete and the LVDT sensors in contact with the stamp at this end measures the horizontal length change. Figure 12 shows the stamp, horizontal LVDT, spacers and bolts inside the U-shaped mold.

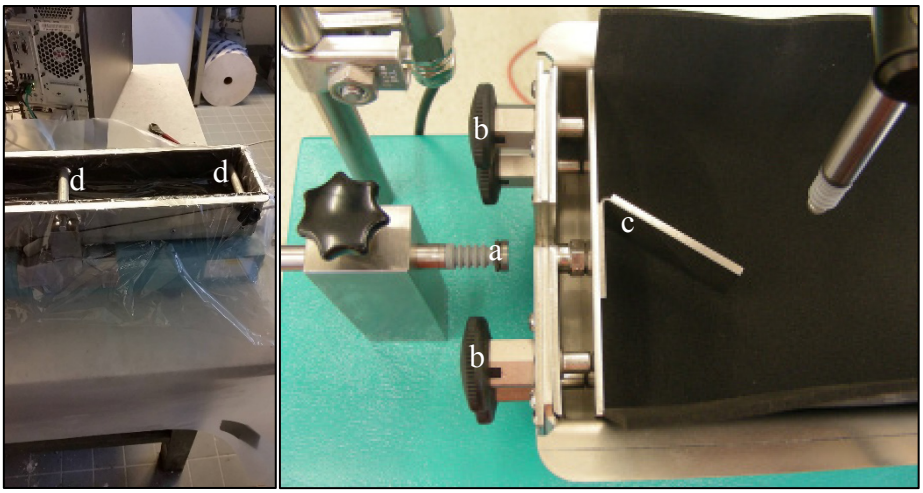

Figure 12 Parts of the Schleibinger Bending-Drain. a) Horizontal LVDT. b) Spacers. c) Stamp/End anchor. d) Bolts/valves.

The stamp/end plate anchor rests on four spacers during filling and compaction of the concrete specimen. The spacers are released to zero position after the specimen has certain strength (approximately 40 minutes after mixing of water). The provided Type K thermocouple is connected to the Bending drain setup with the sensor wires embedded into the specimen. The embedded portion of sensor wires were cut off and reused after each test.

After running the test for 48 hours, horizontal LVDT was removed first. The transverse running bolts are removed next. The specimen is removed with soft hammer strokes if required. The stamp (end anchor plate) and the both valves are then carefully removed from the specimen to use again. The LVDT has a stroke of 5mm and a resolution of 0.3µm.

When spacers are released, the fresh concretes settles (flows) onto the stamp. Development of weak internal structure in the fresh concrete stops this flow and the concrete mass can retain its dimensions. The flow is followed by immediate sharp shrinkage at early hours of the test as explained in next Chapter 5 (Section 5.1.1). This effect was categorized as a test rig artifact in this study, and had been accounted for by zeroing the shrinkage data, also explained in Chapter 5. Section 5.1.1 contains details about data interpretation of early age autogenous shrinkage in this study.

4.4 Drying Shrinkage Test

Drying shrinkage test is a standard test method for measuring dimensional stability of hardened hydraulic-cement mortar or concrete due to changes in the moisture content. Ten concrete mixtures (Table 10) were tested by casting beams with reference studs inside cross-section ends. The test was carried out according to Finnish standard SFS–EN–12617–4(2002) and International standard ISO–1920–8:2009(E). In total thirty beams were cast, three for each mixture type (Section 4.2, Table 10), and cured in a climate room with relative humidity (RH) 65% and temperature 20 ^{o}C. The axial dimensional shrinkage was measured in a control room. The test method is helpful for comparative evaluation of shrinkage in different concrete mixtures.

4.4.1 Test Arrangement

Three beam specimens were prepared to measure the average drying shrinkage for each mixture (Table 10). The specimen dimensions were approximately 100x100x500 mm each. The mold were constructed with a base plate, two end plates and two side plates, which are fastened together. The

end plates act as gauge stud holders. The reference gauge studs were 29mm long. With studs in place in the end plates, the distance between the inner ends of the two studs was approximately 466mm and the distance between the outer ends of the studs was approximately 524mm. Figure 13 shows the mold assembly and stud. Reference studs are held in place using metal wire or clip during the casting of specimens. Table vibration was used for consolidation of concrete. The specimens are cured in the molds (covered with foil) for 24 hours in the laboratory conditions. Before molding the specimens, the contact lines of the mold and base plate and the outside joints are sealed to prevent water loss from fresh specimen. The interior surface of mold is covered with mineral oil for easy demolding.

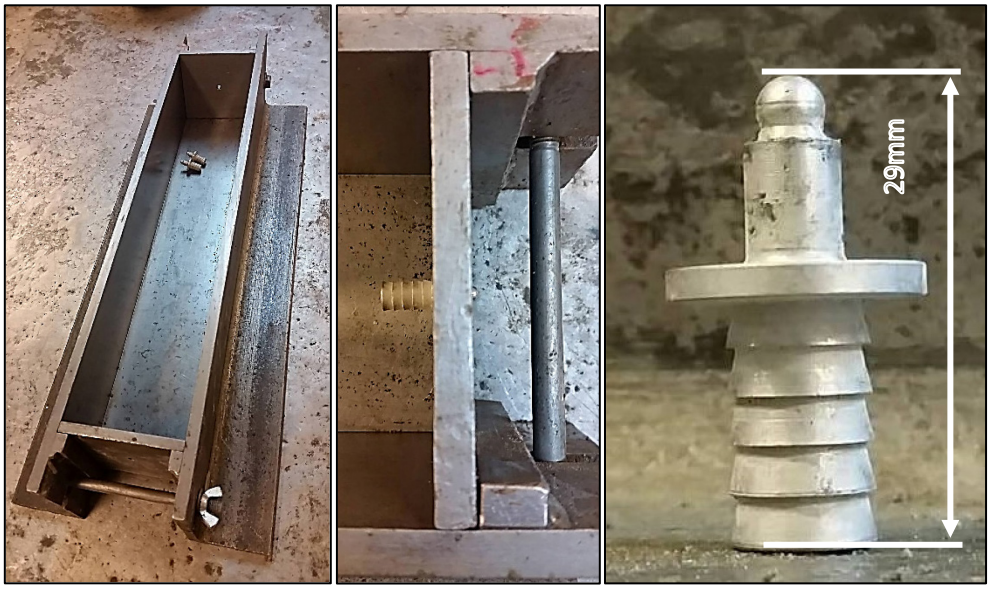

Figure 13 Mold assembly and reference studs for drying shrinkage specimen.

4.4.2 Test Operation

Following 24 hours (±1) curing inside the mold in the laboratory, the specimens were demolded and marked with an identification code and date of casting. The beams specimens were then immediately taken to the climate room for initial measurements. Two types of measurements were taken for each specimen: length readings and weight readings. The frequency of the measurements and the test duration was selected as 1, 3, 7, 14, 28 and 56 days from the day of demolding.

4.4.2.1 Drying Shrinkage Measurement

A vertical length comparator and stainless steel reference bar was used to make the unrestrained shrinkage readings. Both of these items were kept in the same climate room to avoid instrument error due to temperature effects. The vertical comparator was set on an anvil which is kept on top a horizontally leveled table. The apparatus for unrestrained axial length change measurement is shown below in Figure 14.

- Dust is removed from the studs, anvil and grooves of the comparator before measuring the specimen. An alignment point was marked on each specimen to keep same position for each measurements. The measured values of reference bar and specimens were recorded to nearest 0.001 mm.
- The reference bar and the specimen reading is taken consecutively with light force applied to the dial gauge anvil of comparator. The reference bar and specimen was rotated in the grooves of the comparator to ensure that dial reading did not change by more than ± 0.001 mm.

- The reference bar (stainless steel) of 519mm length was placed in the comparator each time a length change reading is taken.
- ***Length Change Calculation*** – The following formula was used to calculate the linear drying change at any age (EN 12617-4:2009(E):

$$Strain = \frac{\Delta L * 1000}{L_g} \left[\frac{mm}{m}\right] \quad \text{Equation 10}$$

where: $\Delta L = (L_x - L_o)$, change in length at age x,
L_o = initial length reading of specimen minus length reading of the reference bar at same time (mm), and
L_x = length reading of specimen at age x minus length reading of the reference bar at age x (mm),
L_g = gauge length is taken at demolding as the distance between the studs (mm).

- Alternatively, strain was also expressed as a percentage, **specific length variation (*c*):**

$$c = \frac{\Delta L * 100}{L_g} [\%] \quad \text{Equation 11}$$

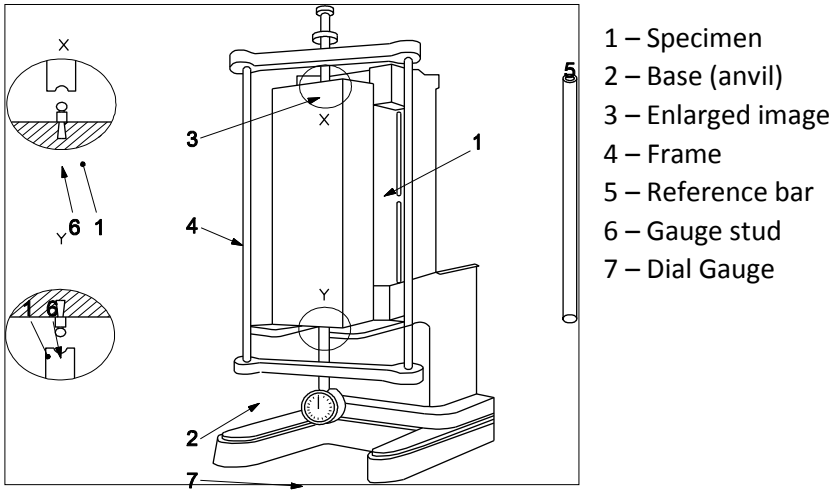

Figure 14 Vertical length comparator (ISO 1920-8:2009).

4.4.2.2 Mass Variation

With each shrinkage measurement, change in mass of the specimen is also recorded at fixed schedule. This mass change can be expressed as **the specific mass variation (*m*)**. Each specimen is weighed and recorded to nearest 0.1 g in order to find loss of water. Concrete with same water to cement ratios are expected to show similar mass variations as homogenous drying conditions are maintained in the drying chamber (climate room). Mass variation at regular intervals is measured to evaluate the influence of fibres, cement type and shrinkage reducing admixture (SRA) on the free shrinkage and water evaporation of fibre reinforced concrete mixtures (FRC).

$$m = \frac{\Delta M * 100}{M_o} [\%] \quad \text{Equation 12}$$

Another way to demonstrate drying shrinkage directly is by calculation of theoretical density at regular time interval. Five-liter volume molds were used to prepare drying shrinkage specimens. The moisture loss can be expressed as loss of water mass per cubic meter of concrete (kg/m^3) on y-axis versus time duration on x-axis.

5 Results and Discussion

In this research, the effect of fibres on the early age shrinkage in autogenous condition and long term drying shrinkage were also evaluated. Fibre reinforced concrete (FRC) samples were designed for the purpose of studying the effect of fibres in concrete both at an early liquid state and in the hardened concrete. The aim of early age testing was to reveal the effects of fibre properties like higher tensile strength, modulus of elasticity, distribution and fibre-concrete bond on the autogenous shrinkage in different concrete samples. To achieve this aim, 0.38% by volume of steel (kg/m^3), plastic (kg/m^3) and fibrillated glass fibres (kg/m^3) were added to three cement types separately. For each cement type, a mixture of comparable plain concrete was also tested to make comparative assessment. Early age autogenous deformation was measured in a shrinkage rig for ten mixtures in a 48–hour test duration. Whereas, long-term drying shrinkage was measured on three prismatic samples for each concrete type in a climate room at 1, 3, 7, 14, 28 and 56 days. To understand the potential effects of fibres on water evaporation, drying was measured by a concept of mass variation. The average of shrinkage and mass variation for the three samples was used to improve the credibility of long-term drying shrinkage results. Within the framework of this work, the influence of a fixed volume of steel, plastic–polypropylene and glass fibres on early age autogenous and long-term drying shrinkage of concrete mixtures was studies. The results of the experiments are presented in the following sections.

5.1 Autogenous Deformation Measurement

Early-age autogenous deformation was measured using Schleibinger Bending-Drain test arrangement as described in Section 4.3. The autogenous deformation of a meter long fresh concrete specimen plotted on the y-axis represents linear horizontal deformation. The deformation is expressed as mm/m. Figure 15 shows a typical test result for cement concrete mixture of w/c = 0.5 and 385 kg/m^3 of Finnsementti plus cement. The measurement for horizontal deformation and specimen temperature is shown in the figure 15.

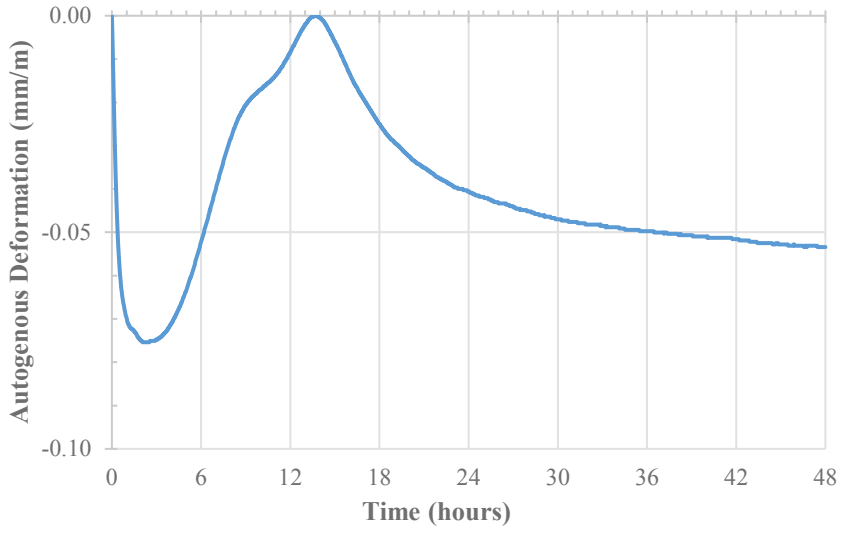

Figure 15 Early age autogenous deformation result.

In the above test results, the values are not altered in any form. They are presented form the start of the test, at approximately 40 minutes from the mixing of water and cement. Large deformation occurs immediately at the start of the test until the age of approximately 2.5 hours. This occurs due to the chemical shrinkage of the cement paste and the settlement of aggregate and cement particles. After

about 2 hours, the rate of shrinkage slows down drastically. This might be attributed to the development of the loose internal skeleton.

The early-age autogenous horizontal deformation measurement can be divided into 3 distinct stages. These stages are marked in the figure 16 and described in the following sections. In Figure 16, x-axis has been magnified, showing only 24 hours, to have a closer look since a lot of deformation activity is happening in the early hours.

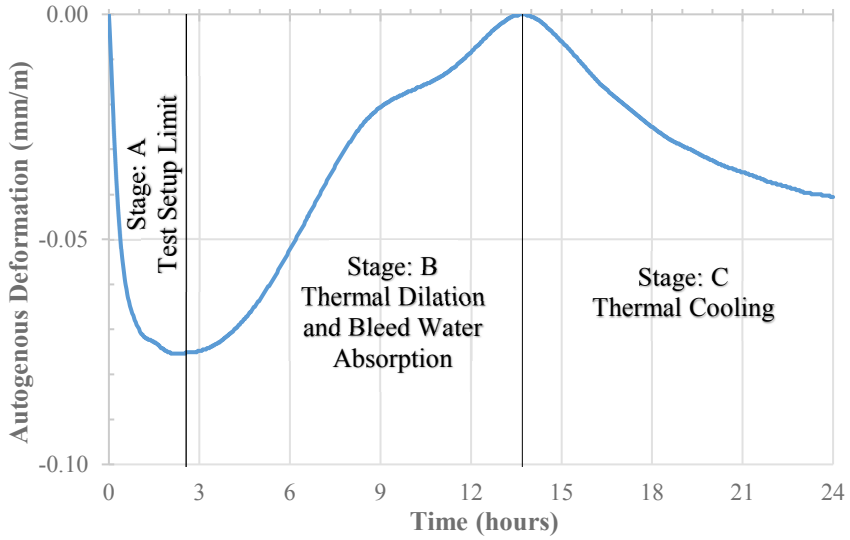

Figure 16 Stages of first 12 hours of the early autogenous deformation result of Figure 15.

- **Stage A: ~ (0 – 2½ hours)**
  At the start of the test, large horizontal shrinkage is recorded. The concrete at this stage is still fluid enough not to induce any harmful stresses due to this shrinkage. However accurate this measurement may be, the equipment's limitations make it questionable. This is termed as an artifact of the test arrangement. As the sample is placed in the U-shaped steel mould, the vertical placement exerts a force on the movable plate, which is partly cast into the sample for detecting horizontal deformation. This excessive early deformation does not exist for stiff or dry (little or no bleeding) mixtures.
- **Stage B: ~ (3 – 14 hours)**
  Thermal effects and bleed water reabsorption cause expansion of the sample from three (3) to twelve (12) hours into the test. Extra bleed water rises to the surface of the concrete sample as aggregates and cement particles settle. After stage A, the bleed water (if any) in this case is drawn back into the sample through the capillary suction allowing the sample to expand. At a time when bleed water is completely absorbed into the concrete sample, the on-going hydration develops capillary pressure rise that is understood to be a main cause of early-age autogenous shrinkage deformation. However, in this case, the bleed water reabsorption coincides with thermal expansion phase due to which capillary pressure-controlled shrinkage is not observed clearly. Hydration reaction-controlled thermal expansion exceeds the capillary suction and causes large expansion.
- **Stage C: ~ (14 + hours)**
  At the end of hydration heat generation, the sample starts cooling which results in contraction of the concrete sample. The shrinkage during this continuing stage is somewhat exaggerated due to the cooling effect. However, as the concrete sample reaches the room (curing) temperature, shrinkage deformation continues at a much slower rate. With the progression of

hydration, water availability becomes lesser within the microstructure of concrete sample, and capillary suction contributes to the autogenous shrinkage deformation.

5.1.1 Data Interpretation

The test result for the early-age autogenous horizontal deformation consists of various stages as explained in the previous section. These stages essentially show the effects of various factors during physical evolution of the concrete sample. Moreover, for the comparisons of different concrete, it is important to have a *reference point*. Holt (2001) suggests three approaches, which may be used to evaluate the early-age autogenous deformation results for the aim of comparison. Each approach is purpose-based and provides a unique utility for concrete experts. The purpose of testing governs the selection of interpretation method. Based on the approaches, we may have a scientific, engineering or a structural reference point.

- **Scientific** reference point requires the complete evaluation of results from the time when test begins. This approach prohibits any kind of alteration to the test result values. Following this approach, the reference point is obtained by zeroing at the start of the test results. The main purpose of the test is to explain fundamental principles influencing the deformation experiment. This method allows qualitative explanation of the test results.
- **Structural** approach is more dependent on the test setup arrangement. The purpose of this approach is to simulate the actual field conditions. Therefore, the results are not corrected or manipulated for the thermal effect. Both the material properties and field constraints are incorporated into this approach. The reference point is case-specific for the structural approach. For this experiment, the reference point is obtained by zeroing at the start of thermal cooling. The reason being that stresses from expansion are relieved during the cooling stage. This approach allows for both qualitative and quantitative data interpretation.
- **Engineering** viewpoint requires data interpretation to draw conclusive results for all materials. According to this approach, the test results are used to provide a benchmark for using concrete. The constraints of test setup such as temperature-controlled deformation are corrected before comparison of results can be made. The results solely reflect the material behavior. The engineering reference point for this experiment is at the start of thermally controlled expansion at the end of stage A. Somewhere during stage B, the bleed water (if any) is reabsorbed and the concrete sample keeps on expanding due to hydration temperature. In the absence of bleed water, the reference point should correspond to the physical state when the concrete is no more fluid and any length changes may induced harmful stresses to the concrete.

For this experiment, the magnitude of the autogenous deformation is of importance as a basis of comparison. Henceforth, engineering-viewpoint for data interpretation is used for of results.

5.1.2 Effect of Hydration Heat and Bleed water

Bleed water appears on the surface of concrete sample in the Bending-Drain. This water rises to the top surface as the concrete settles. For most experiments, bleed water has been visually observed at about approximately 2½ hours from the start of the test. This bleed water is absorbed back into the concrete sample due to autogenous conditions and swelling is recorded. At the same time thermal effect of hydration heat start to appear as expansion of the sample in mold, therefore, exclusive effect of bleed water reabsorption is not recorded in this experiment. While ascertaining bleed water reabsorption or thermal effect as the cause of swelling, it important to note that swelling causes compressive strains, in effect acting against shrinkage.

The large amount of heat generated during hydration influences the reference point selection. For engineering viewpoint interpretation, thermal dilation need be removed from the test measurement. True autogenous deformations can be generalized for a material only after making such corrections, and then zeroing the results as explained in Section 5.1.1. The temperature history for the concrete mixture of Figure 15 is shown below in Figure 17 with temperature on the right y-axis and autogenous deformation on the left y-axis.

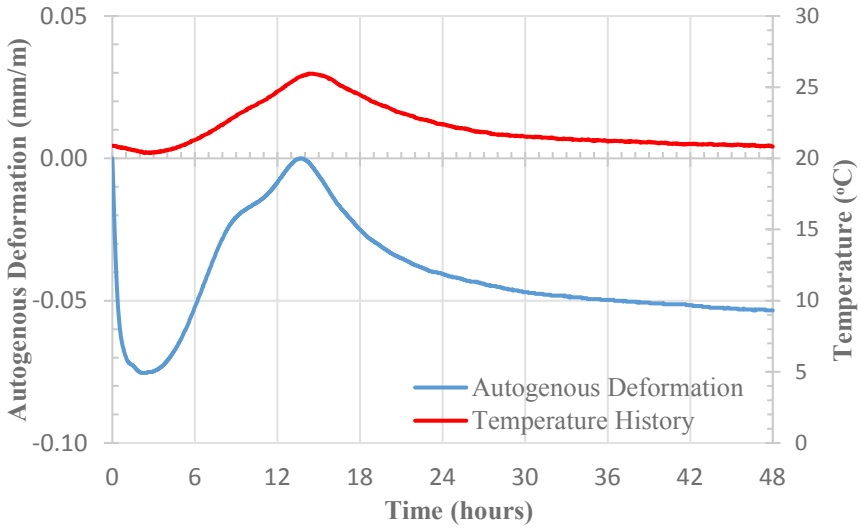

Figure 17 Autogenous Deformation and Temperature development over time from start of test. w/c = 0.5 with superplasticizer 0.37%

The concrete sample recorded a maximum temperature of 26°C at 14 hours. The heat of hydration begins developing at about 3 hours for Finnsementti plus cement and causes significant thermal expansion. It is difficult to measure thermal expansion of concrete at early age. Hedlund (1996) had measured a value of approximately 25 microns/°C for concrete at the age of 10 hours. Equation 14 used to estimates the thermal expansion coefficient (TEC) of concrete during the early ages in this work (Holt, 2001), shown in Figure 18. It should be noted that equation 14 is valid between 3-24 hours of experiment time. Constant values are considered outside these limits.

$$TEC = 193.9 * t^{-0.86} \qquad \text{Equation 14}$$

where: TEC = thermal expansion coefficient, (μ/°C), and
t = time, hours.

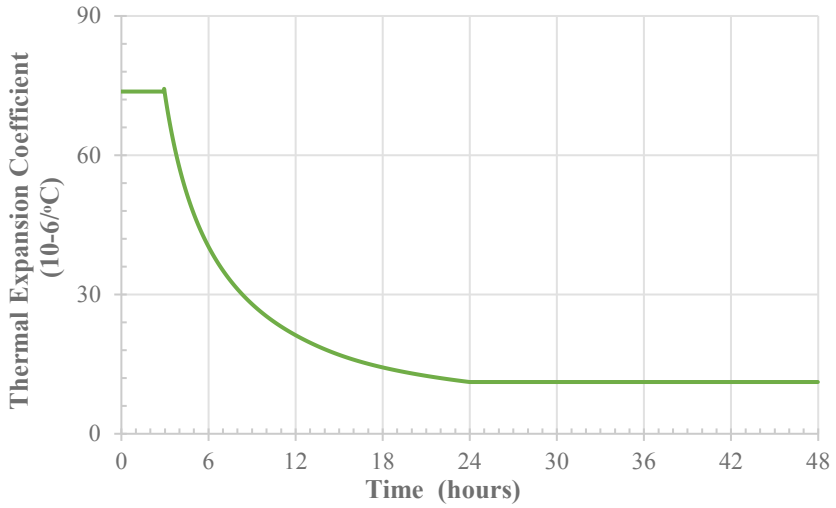

Figure 18 Thermal expansion coefficients for concrete. (Hedlund 1996, Holt 2001).

The TEC is adjusted for each mixture based on the maturity concept. This helps to correct and take into account the temperature and strength development. The concrete age was adjusted according to equation 15 taken from CED-FIP MODEL CODE (1990). This equation is valid for concretes made of Portland cements or cements containing only low amounts of components other than Portland cement clinker.

$$t_T = \sum_{i=1}^{n} \Delta t_i \exp\left[13.65 - \frac{4000}{273 + \frac{T(\Delta t_i)}{T_0}}\right] \qquad \text{Equation 15}$$

where: t_T = temperature adjusted concrete age.
Δt_i = number of hours where a temperature T prevails.
$T(\Delta t_i)$ = temperature during the time period Δt_i.
T_0 = 1°C.

From this maturity adjusted TECs and temperature history of concrete specimen, thermal expansions are calculated. Figure 19 shows the temperature on left y-axis and thermal expansions on right y-axis, thus calculated by multiplying TECs with temperature differences.

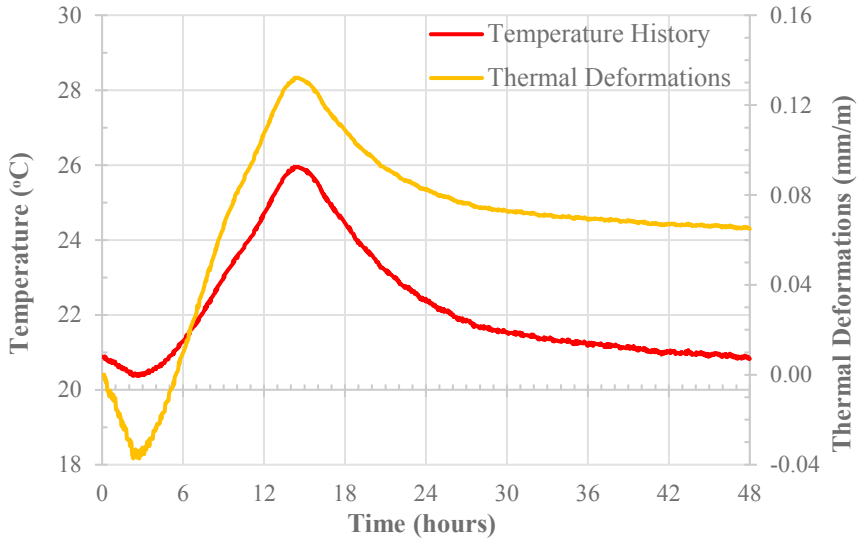

Figure 19 Temperature development and consequent thermal deformations calculated from maturity-adjusted thermal expansion coefficient of Figure 18.

Maturity-adjusted thermal deformations provide basis to implement the engineering viewpoint of data interpretation. Thermal effects are factored out from the raw result of values of so-called autogenous shrinkage of Figure 16 and Figure 17. Expansion of 0.13 mm/m can be expected due to cement hydration thermal effects. Another important fact to notice is that the contraction magnitude due to cooling is almost half that of expansion due to heating. This is due to the decreasing TECs as seen in Figure 18. The early-age horizontal autogenous shrinkage is corrected following the development of thermal deformation calculation. Figure 20 shows the raw values of horizontal shrinkage from the Bending-drain test, the corrected shrinkage following the thermal expansion corrections and zeroed-corrected autogenous shrinkage deformation (zeroed at start of stage-B as explained in Section 5.1.1). This new corrected autogenous shrinkage is necessarily isothermal i.e. if the test setup was cooled externally to take away cement hydration heating.

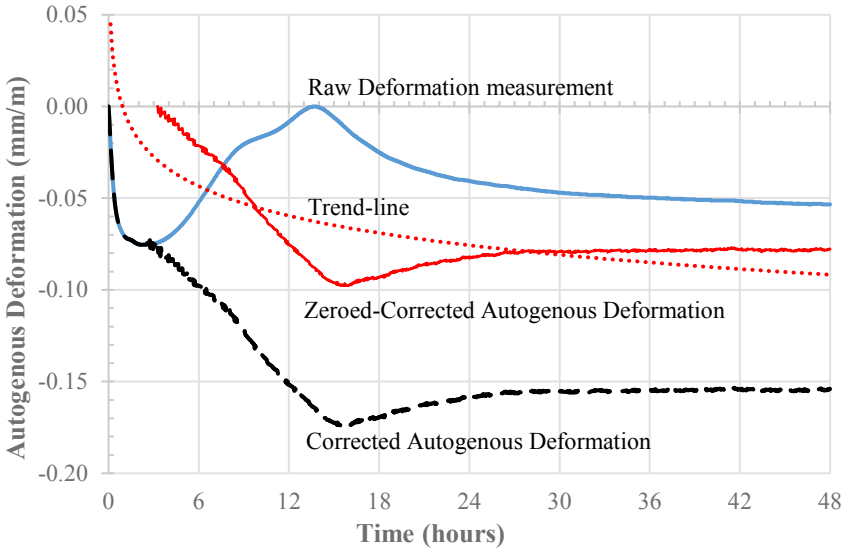

Figure 20 Measured Autogenous Deformation and Corrected Autogenous Deformation.

The black dashed line shows the true autogenous deformation. After approximately 3 hours, thermal expansion effect exceed shrinkage forces and an overall expansion is registered in measurement. Thermal expansion of the stainless steel U-shaped mold, estimated to be $17(10)^{-6}/^{o}C$, also allows for some expansion space for concrete sample (Gere & Timoshenko, 1990). However, there is still some friction offered by the mold walls, which restrains the concrete, both in expansion and contraction. It should be noted that thermal deformation during cooling are subtracted from the overall shrinkage, otherwise the shrinkage measurement would be exaggerated due to the thermal contraction effect. Saje et al. (2012) have suggested in their findings that the initial temperature of the test specimens has effect on the time of start of autogenous shrinkage. However, the same effect was not on the size of the autogenous shrinkage of each test (Saje, et al., 2012). Since all the test samples were prepared on separate days, the initial temperature at the beginning of the measurement was different. Figure 20 shows that corrected autogenous shrinkage would be greatest (0.175 mm/m) at about 16 hours from test start. In the corrected autogenous shrinkage graph, the sample seems to contract slightly after peak shrinkage value. This is limitation of the applied correction procedure. The real isothermal autogenous shrinkage would be similar to the red dotted logarithmic trend-line.

This method of engineering viewpoint data interpretation of autogenous shrinkage show that beam shrinkage measurements of Bending-drain underestimate shrinkage due to thermal expansion. Similarly, the above procedure need be applied to other tests as well for making generalized comparisons regarding the tested materials.

5.1.3 Effect of Different Type of Fibres

There is a general agreement among researchers that the addition of fibres to concrete can have reducing effect on the so-called interior strain (due to autogenous effects) and the thermal expansion coefficient (TEC). The fibres disrupt the interconnection of pores, reducing the overall water content in the capillary pore (Lei & Cao, 2011). Fibres are known to affect thermal deformations also. Increasing dosage of fibers in the concrete will reduce the overall TEC of FRC. The behavior of fibres in crack control has already been explained in Section 2.4.1. The elastic modulus of fibres being higher than that of concrete and higher strength-to-size ratio both contribute in reducing the concrete deformation as compared to the plain concrete. Fibres also have much lesser linear expansion potential than fluid concrete at early age. Lei and Cao (2011) have experimentally demonstrated that fibres having higher modulus reduce the TEC of concrete more than fibres with lower modulus.

The measured results of the shrinkage rig test (Bending-Drain) consisted of consisted of both autogenous and thermal deformations over the time of 48 hours (Section 5.1.2). The influence of temperature variations were calculated analytically from TEC. Adjustment for thermal deformation was made to the measured autogenous shrinkage from the test data. The zeroed-corrected 48 hours autogenous deformation (along length) and temperature history (at the middle of specimen height) of Plus, SR and White cement concrete mixtures are shown in Figures 21, 22 and 23. It was observed that the fibre reinforced concretes behaved similarly to plain concrete in the first few hours of the test. However, there were noticeable difference in the maximum and 48 hour autogenous shrinkage (AD) values. The AD of fibre reinforced concrete was found to be lesser than that of plain concrete mixtures for all three types of cement mixtures. It might be because of the fact that fibres reduce the AD when they are subjected to the shrinkage-induced tensile stresses, by shear along the fibre-matrix interface (Mangat & Azari, 1984).

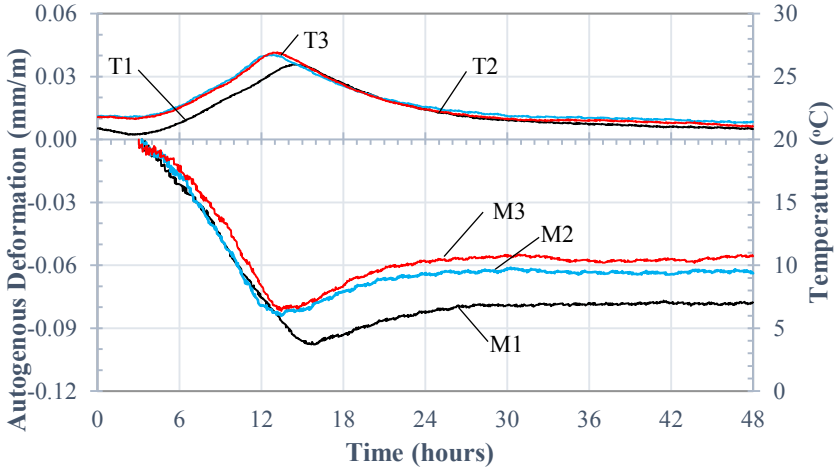

Figure 21 Autogenous Deformation (AD) and Temperature history of Plus cement concrete mixtures, M1 (Plain Concrete), M2 (Steel Fibre Concrete) and M3 (Plastic Fibre Concrete) with 0.38% fibre volume.

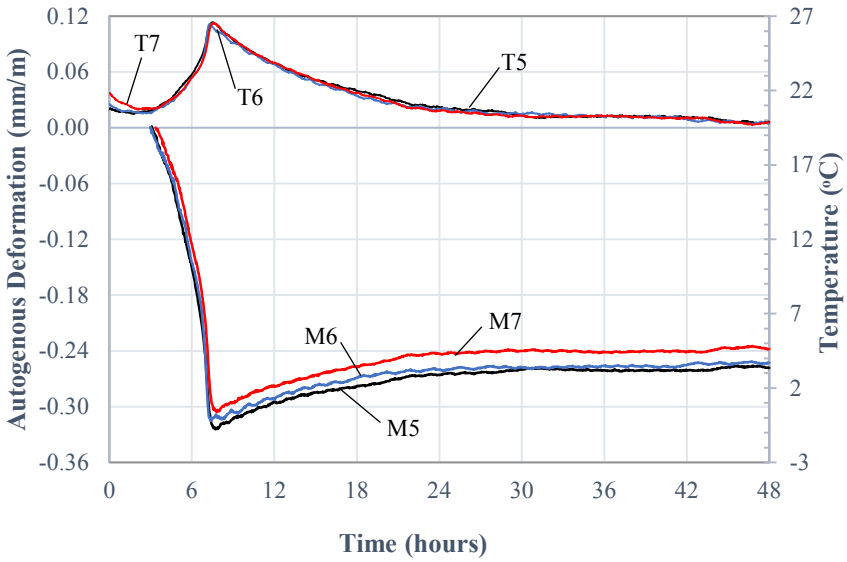

Figure 22 Autogenous Deformation (AD) and Temperature history of White cement concrete mixtures, M5 (Plain Concrete), M6 (Plastic Fibre Concrete) and M7 (Glass Fibre Concrete) with 0.38% fibre volume.

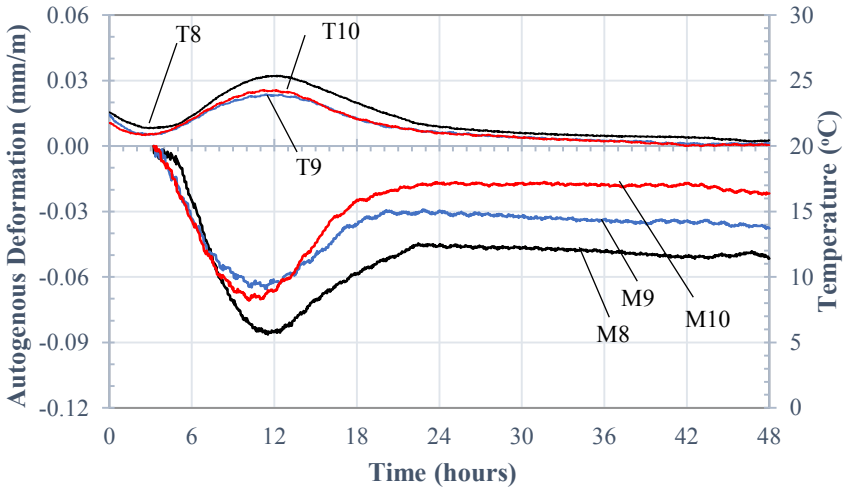

Figure 23 Autogenous Deformation (AD) and Temperature history of Sulfate Resisting (SR) cement concrete mixtures, M8 (Plain Concrete), M9 (Steel Fibre Concrete) and M10 (Plastic Fibre Concrete) with 0.38% fibre volume.

- Plus cement concrete mixtures (Figure 21):

From the presented results in the Figure 5.7, it can be seen that the early age autogenous deformation of plain concrete was greater than with the fibres. The maximum AD of 0.38% steel fibre concrete was approximately 14% less than AD of the plain concrete. Moreover, the maximum AD of 0.38% plastic fibre concrete was approximately 16.5% lesser than the maximum AD of the plain concrete. At the end of test at 48 hours, the AD of steel fibre concrete was approximately 18% less and the AD of plastic fibre concrete was approximately 28% lesser than the AD of the plain concrete mixture. It can be said that, with same dosage of fibre volume, plastic (polypropylene) fibers reduce the early age AD greater than steel fibres.

- White cement concrete mixtures (Figure 22):

Figure 5.9 presents the early age AD results for White cement concretes. The maximum AD of plain White concrete was greater than with the use of fibres. Maximum AD for 0.38% plastic fibre concrete was approximately 3% less than maximum AD of the plain white concrete. Whereas, the maximum AD for 0.38% glass fibres was approximately 6% less than the AD of plain white concrete. The fibrillated glass fibres performed almost twice as good in reducing shrinkage as the plastic fibres in case of White cement concrete. However, there was not much difference in total AD of plain or fibre concrete for White cement. It can be said that, for the range of fibre content used in this work for White cement concrete, the fibres did not have a considerable effect on AD like the case of Plus and SR fibre reinforced concrete mixtures.

- Sulfate Resisting (SR) cement concrete mixtures (Figure 23):

The early age AD of SR plain concrete was greater than with the addition of fibres. The maximum AD of 0.38% steel fibre concrete mix was approximately 24% less than that of maximum AD of plain concrete mix. The maximum AD for 0.38% plastic fibre concrete was found to be approximately 18% less than the maximum AD of the plain concrete mix of SR cement. At 48 hours, the AD of steel fibre concrete was approximately 27% less, and that of plastic fibre concrete was approximately 57% lesser than that of the plain SR cement concrete. The plastic fibres reduce the early age AD more than the steel fibers in the case of SR cement concrete too.

The results show that the addition of 0.38% by volume of fibres had an overall reducing effect on the autogenous deformation of the shrinkage rig specimens, regardless of the magnitude of the

deformations. The plastic-polypropylene (Master Fibre 246) reduced the early age autogenous deformations at 48 hours by 28%, 57% and 3% of the plain concrete mixtures for the Plus, SR and White cement, respectively. The steel fibre (HE1/50) reduced the early age autogenous deformations at 48 hours by 18% and 27% of the plain concrete mixtures for Plus and SR cement. Moreover, the fibres were apparently more effective in SR cement concrete mixtures. For the same fibre volume of 0.38%, greater number of the plastic-polypropylene fibres had almost twice the reducing effect on early age AD as compared to the heaver steel fibres for Plus and SR cement concrete mixtures. Previous research work have also established that the plastic-polypropylene fibres are more effective in eliminating shrinkage than steel fibres (Sandbakk, 2007; Saje, et al., 2012; Zollo, 1996).

Glass fibres reduced the early age AD for white cement concrete by 6%, approximately twice than that of plastic fibres. One reason for better performance of the glass fibres (Anti-Crack HP 24) could be the better dispersion in the mixture due to a specific weight similar to the concrete. As a result, the fibrillated glass fibres are known to be better dispersed in the concrete mixture.

5.1.4 Effect of Shrinkage Reducing Admixture (SRA)

The use of shrinkage – reducing admixture (SRA) in concrete reduces the surface tension of the water mixed in concrete in an effective way to reduce the volume instability phenomenon of shrinkage (Tazawa & Miyazawa, 1995; Lura, et al., 2007; Ruacho, et al., 2009). To demonstrate this effect, 1% (by weight of binder) dosage of BASF MasterLife 815 SRA was added to steel fibre reinforced concrete (SFRC) using Plus cement. Comparative study of the early age autogenous deformation (AD) with the shrinkage rig test revealed that SRA was effective in reducing the early age AD of the SFRC. The use of steel fibres already proved to reduce the AD compared to the plain concrete (Section 5.1.3). The addition of SRA also had a reducing effect on the early age AD. Mora-Ruacho et al. (2008) demonstrated in their research that SRA reduces the driving forces of shrinkage: decreasing the surface tension of the mixing water during the early age fluid phase, lowering evaporation rate (drying condition), and delaying the rise of capillary pressure (Ruacho, et al., 2009). Figure 24 shows the comparison between zeroed-corrected AD of two mixtures of SFRC (Section 3.2), with and without 1% SRA.

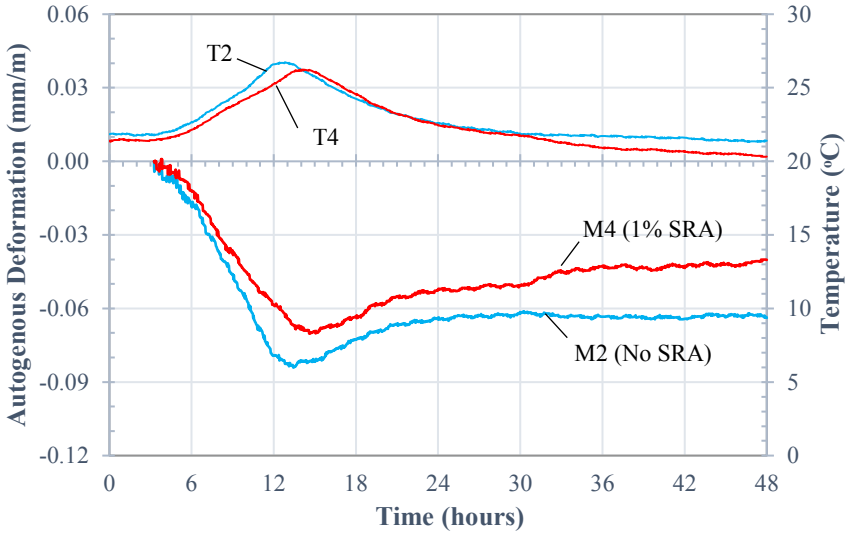

Figure 24 Shrinkage Reducing Admixture effect on Autogenous Deformation (AD) and Temperature history of steel fibre reinforced concrete mixtures, M2 (Steel Fibre Concrete without SRA), M6 (Steel Fibre Concrete with 1% SRA).

A noticeable feature in Figure 24 is the delayed peak temperature rise and delayed maximum early age AD with the use of SRA. This side effect has been reported in previous studies and mentioned in

the manufacturer's product documents. However, the perceived delay is within 1-hour period. The use of SRA reduced the maximum early age AD of SFRC by approximately 16.5%. Whereas, the reduction of early age AD at 48-hours was greater than 37%. However, the mixture containing 1% SRA showed greater workability (slump) and apparently more free water. This is a direct effect of reduced surface tension of the mixing water in the liquid stage.

5.1.5 Effect of Cement Type

Figure 25 shows the changes in autogenous shrinkage for plain concrete samples of the Plus, White and SR cement types. These results were zeroed and corrected according to structural viewpoint as explain earlier in Section 5.1.2. M1 and T1 represent Plus cement concrete, M5 and T5 represent White cement concrete and, M8 and T8 represent SR cement concrete (Section 4.2, Table 10). Same mixture design was used for Plus and SR cement types, with w/c ratio of 0.50. However, for White cement concrete, a w/c ratio of 0.55 was used with four limestone 22R aggregate factions, more than twice amount of filler and maximum aggregate size of 12mm.

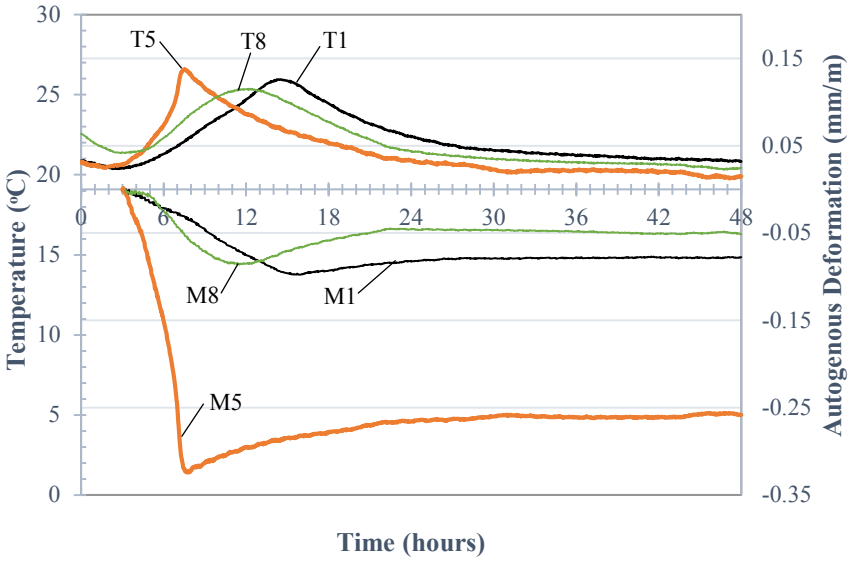

Figure 25 Comparison of Autogenous Deformation (AD) and Temperature History of Plain concretes with Plus, Sulfate Resisting and White Cement Concrete.

The different clinker compositions and initial setting times of the cement types also reflected in the thermal changes as seen in the temperature history. In Figure 25, the shrinkage data was referenced at the start of thermally controlled deformations. The mixture (M5) showed less bleed-water and the concrete was sticky. After the peak temperature during hydration, rapid shrinkage was observed with white concrete mixtures. Part of this early age autogenous shrinkage was understood to be due to thermal cooling and adjusted accordingly as explained in Section 5.1.2. Other mixtures with Plus and SR cement exhibited thermal expansions exceeding the amount of early age shrinkage. Recall form materials section (Section 3.1 Cements), the Plus cement clinker had higher limestone and slag addition that has resulted in delayed maximum heat generation and slower hydration. The SR cement had an earlier heat peak but even lower heat generation compared to both Plus and White cement concretes. This is evidence of the lesser C_3S and C_3A content.

Apart from the maximum magnitudes of the mixture temperatures and autogenous deformations, it can be seen that these temperature histories and autogenous deformation measurements are characteristic in nature. Qualitatively, they represent the material properties of the corresponding cement type mixture and the test arrangement. The temperature histories (T1 for Plus, T5 for White & T8 for SR) of plain concrete mixtures suggest that hydration reactions occur in a different way in

these cement types. The high early heat of hydration causes thermal swelling in Plus and SR cement type mixtures. Whereas, it only resists the autogenous shrinkage deformations in the White cement mixtures. The thermal effects were removed from the raw autogenous deformation data using maturity adjusted TEC. The corrected results confirm the same logic as White cement mixture type showed large amounts of corrected autogenous shrinkage deformation, followed by Plus and SR type mixtures.

The engineering viewpoint autogenous shrinkage data shows that maximum deformation occurs at about peak temperature. As shown in Figure 25, maximum early-age AD occurred for White cement concrete, while SR cement concrete showed the least deformation. Whereas, the early age AD for the Plus cement concrete was greater than the SR cement type mixture, both maximum and at 48-hour time. The plain white cement concrete had approximately 70% and 73% greater maximum autogenous deformation and, approximately 70% and 80% greater autogenous deformation than Plus and SR type plain concrete mixtures at 48–hour, respectively.

The SR type plain concrete mixture (M8) had approximately 12% and 34% lesser autogenous deformation at maximum and 48–hour instances compared to the Plus type plain concrete mixture (M1). Another comparison has been made between Steel Fibre Reinforced Concrete (SFRC) mixtures (M4 and M9). Mixture M4 had Plus type cement with 1% SRA, whereas mixture M9 had SR type cement without SRA. From engineering viewpoint, Figure 26 shows that the maximum and 48–hour autogenous deformation for SFRC for the Plus cement is quite close to SFRC mixture with SR cement and no SRA dosage. The maximum and 48–hour autogenous deformation of SFRC of SR cement and no SRA is approximately 7% and 6% lesser than SFRC of Plus cement with 1% SRA. Therefore, Plus cement mixtures exhibit greater autogenous deformation than SR cement mixtures, both in plain concrete mixtures and fibre concrete mixtures. The effect of SRA off-settled the autogenous deformation in Plus cement close to that of SR cement. This effect is congruous to the explanation in Section 5.1.4 (Figure 24).

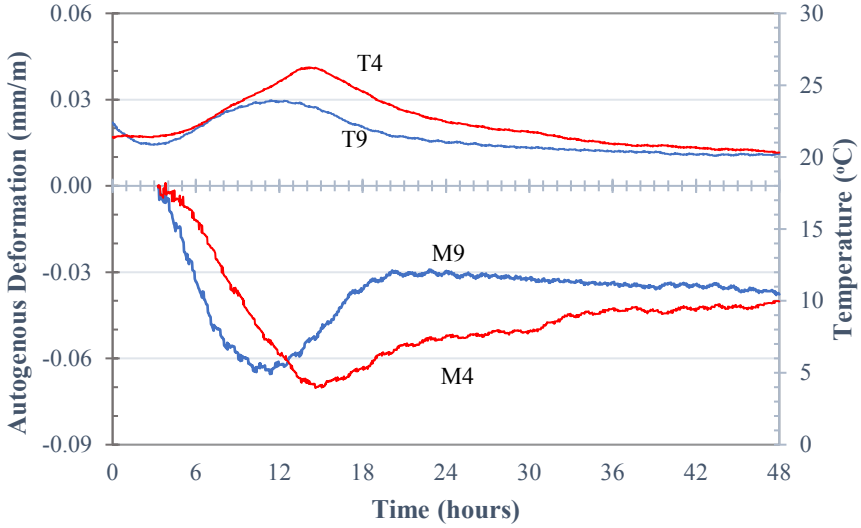

Figure 26 Comparison of Autogenous Deformation (AD) and Temperature History of Steel Fibre Reinforced Concretes with Plus cement with SRA (T4 & M4) and Sulfate Resisting cement without SRA (T9 & M9).

The temperature development was also affected by the ambient condition (temperature-controlled room) and size of concrete specimen in this work. As we know that, massive concrete structures with large cross-sections would have a different temperature profile. Owing to the size effect, there is probability of temperature gradients in the same cross-section of concrete, causing relative strains in

different layers of the cross-section. Moreover, heat dissipation in concrete members with large cross-section is also much slower. The effect of thermal deformations in the industrial construction is expected to be greater on the overall autogenous deformations. Consequently, the calculation method of early-age deformations should also consider the factors such as the size and shape of the specimen.

5.2 Drying Shrinkage Measurements

The unrestrained axial length shortening was measured manually using comparator system with a reference bar. The test specimens were demolded after 24 hours, and then exposed to a constant environment of the climate room with a constant temperature of 20°C and RH 65%. A reference value for the sample weight and initial length was measured on the day of demolding. The procedure and calculations for the drying shrinkage measurements are explained in Section 4.4. The results of linear drying shrinkage are presented in the units of mm/m on y-axis vs time duration in days on x-axis. For each concrete mixture, average values of three samples were taken as representative for both linear drying shrinkage and average water loss. This averaging was done to remove fluctuation in the measurement as the properties of fresh concrete are sensitive and are affected by mixing, placing, casting and ambient conditions. The drying shrinkage results for plain and fibre reinforced concrete for each cement type are presented in Figure 27, 28 and 29.

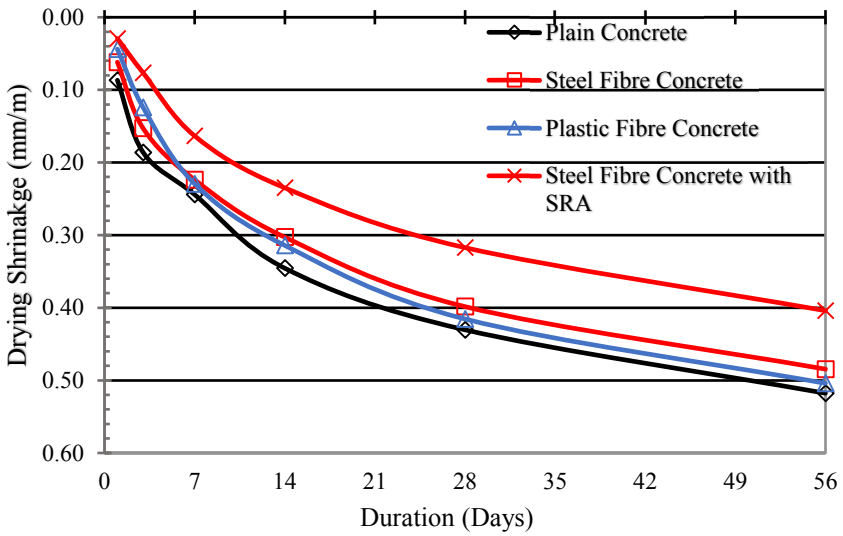

Figure 27 Comparison of Drying Shrinkage for concretes with Plus cement at w/c ratio of 0.50. M1-Plain concrete, M2-Steel fibre concrete, M3-Plastic fibre concrete and M4-Steel fibre concrete with SRA.

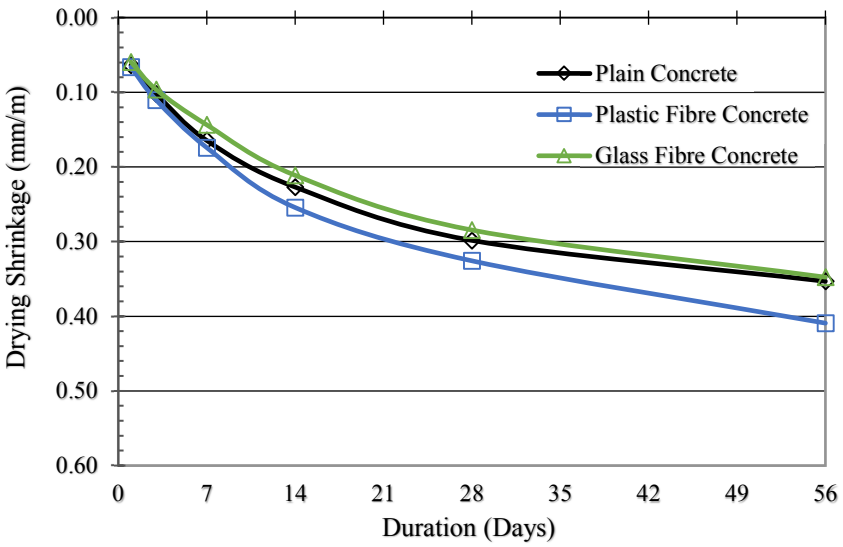

Figure 28 Comparison of Drying Shrinkage for concretes with White cement at w/c ratio of 0.55. M5-Plain concrete, M6-Plastic fibre concrete, M7-Glass fibre concrete.

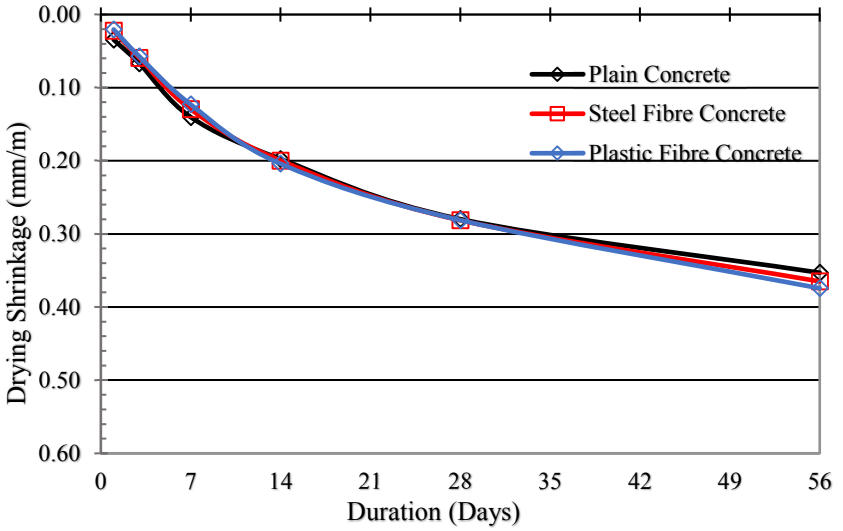

Figure 29 Comparison of Drying Shrinkage for concretes with SR cement at w/c ratio of 0.50. M8-Plain concrete, M9-Steel fibre concrete, M10-Plastic fibre concrete.

5.2.1 Fibres and Cement Type Effect

1. Plus cement concrete mixtures (Figure 27):

The time history for unrestrained drying shrinkage of plain concrete and fibre reinforced concrete showed negligible difference. Moreover, the average drying shrinkage of plastic fibre concrete samples was slightly greater than steel fibre concrete and plain concrete samples for Plus cement concrete mixtures. However, the steel fibre concrete with the use of 1% weight of binder of SRA (M4) exhibited approximately 17% less drying shrinkage than steel fibre concrete mixture (M2) without SRA.

2. White cement concrete mixtures (Figure 28):

The drying shrinkage results for White cement concrete mixtures were almost same for plain concrete, and plastic and glass fibre concrete mixtures. Overall, these drying shrinkages were also comparable to the drying shrinkage measurements of Plus and SR concrete mixtures, unlike in the early age

autogenous deformation measurement. Fibres seem to have little effect on the drying shrinkage of the concrete mixtures in the hardened state.

3. Sulfate Resisting (SR) cement concrete mixtures (Figure 29):

For plain and fibre concrete samples, no notable difference in the drying shrinkage was recorded at the end of 56–day measurement schedule. drying shrinkage of steel fibre concrete mixture of SR cement (M9) is approximately 10% less than the plus cement steel fibre concrete mixture with 1% SRA (M4). The trend for SR cement concretes exhibiting lesser shrinkage deformation than Plus cement concretes remained the same for both early age autogenous deformations and long-term drying shrinkage. Hence, it can be said that in general, Plus cement concrete are more prone to shrinkage effects than SR cement concrete mixtures.

The dosage of fibres used seem to affect the early age AD but not the long-term drying shrinkage in amounts used in this work. A plausible discussion is that the greater stiffness of the steel fibres, and slightly lesser of the plastic fibres, are relatively high in comparison to the young liquid concrete sample at the early age. Due to this, the effect of fibres on the general properties of the fresh concrete is greater than in later periods of hardening. A higher amount of drying shrinkage in white plastic fibre concrete can be explained because of increased porosity causing greater moisture loss compared to white glass fibre concrete and plain white concrete. The same explanation was also given by Aly et al. (Aly, et al., 2008). However, this explanation cannot be applied to overall results of fibre concrete mixtures in this work.

5.2.2 Mass Variation from Water Loss

The drying shrinkage of hydraulic cement composites depend largely on the water permeability of the concrete samples. Saje et al. (2012) have summarized that the addition of longer steel fibres increased the water permeability more than by the addition of short steel fibres (Saje, et al., 2012). Overall, the principle was stated that fibres acted as bridges between the pores allowing for easier escape of water. Wongtanakitcharoen and Naaman (2006) have regarded the effect of fibres on the loss of free water as a key element to understand drying shrinkage of fibre concretes. The principle of pore bridging could not be established by the measurement results in this work. The mass variation from water loss was measured at same time as the drying shrinkage. The mass variation, expressed as water loss on y-axis (kg/m^3) with time duration in days on x-axis (hours) is presented in Figure 30, 31 and 32.

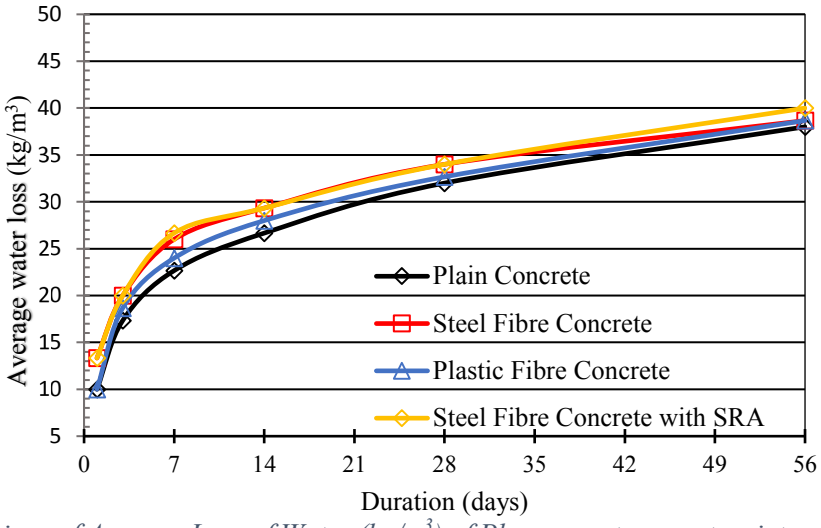

Figure 30 Comparison of Average Loss of Water (kg/m^3) of Plus cement concrete mixtures at w/c ratio of 0.50. M1-Plain concrete, M2-Steel fibre concrete, M3-Plastic fibre concrete and M4-Steel fibre concrete with 1% SRA.

The steel fibre concrete mixtures with and without 1% SRA dosage for Plus cement concrete mixtures (M2 and M4) exhibited slightly greater mass variation at 7th and 14th–day measurement. However, for the 56th day measurement of mass variation, no notable different of average water loss was recorded between fibre concrete mixture samples and plain concrete mixture samples. This trend was constant for the mixture types belonging to each cement type.

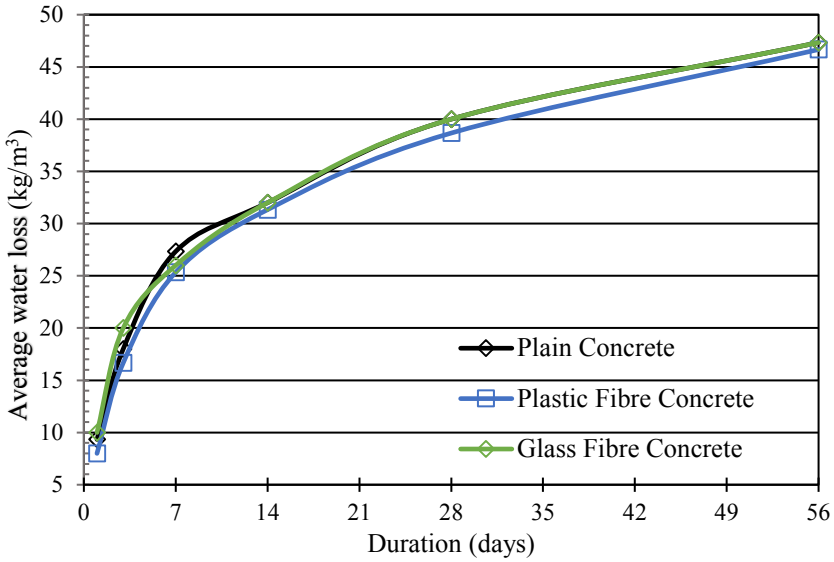

Figure 31 Comparison of Average Loss of Water (kg/m3) of White cement concrete mixtures at w/c ratio of 0.55. M5-Plain concrete, M6-Plastic fibre concrete, M7-Glass fibre concrete.

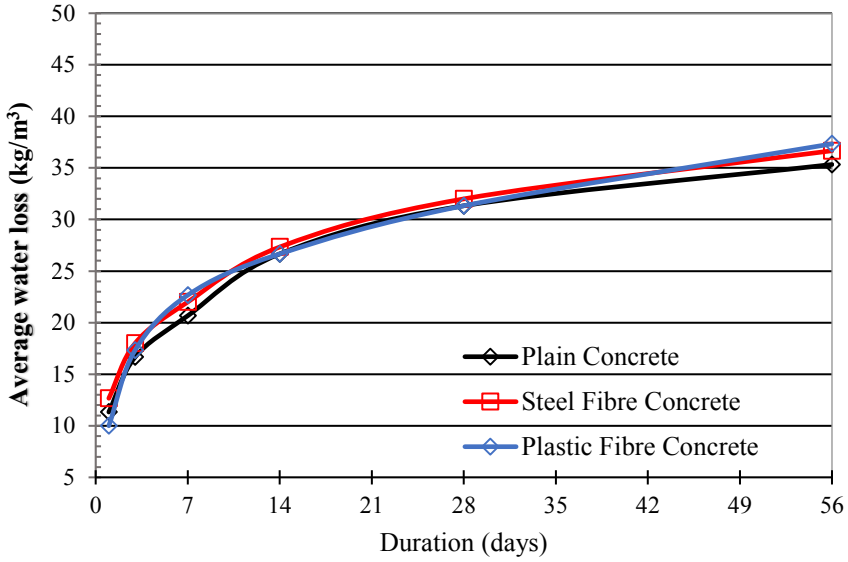

Figure 32 Comparison of Average Loss of Water (kg/m3) of SR cement concrete mixtures at w/c ratio of 0.50. M8-Plain concrete, M9-Steel fibre concrete, M10-Plastic fibre concrete.

The increase in water permeability causing greater drying shrinkage was not observed in this study with a fibre volume of 0.38%. However, despite slightly lower w/c ratio, white cement concrete exhibited a greater specific mass variation than concrete mixtures of Plus and SR cement types. Nevertheless, with a dosage of 0.38% by volume of fibres, no noticeable difference was measured between plain concrete mixture and fibre concrete mixture samples of White cement. The average weight loss of plain White cement concrete samples was recorded to be approximately 19% and 25% greater than plain Plus and SR cement concrete samples at 56-day, respectively.

For all the test samples, the addition of fibres produced neither a clear effect nor any significant change to the drying shrinkage measurement and mass variation from water loss. Thus, the addition of fibres at 0.38% by volume does not affect the loss of moisture from concrete to surroundings.

5.3 Total Early Age Autogenous Deformation and Long-term Drying Shrinkage

The early-age autogenous deformation and long-term drying shrinkage are combined to present a general understanding of the results. This combined representation of two experiment series also give a comparison between the magnitudes of early-age and long-term linear deformations of concretes with same composition. The relation between autogenous and drying effects is not simple and clear, as the driving forces causing each phenomenon are different. Figure 33, 34 and 35 show the total deformations for Plus, White and SR cement concrete mixtures, respectively.

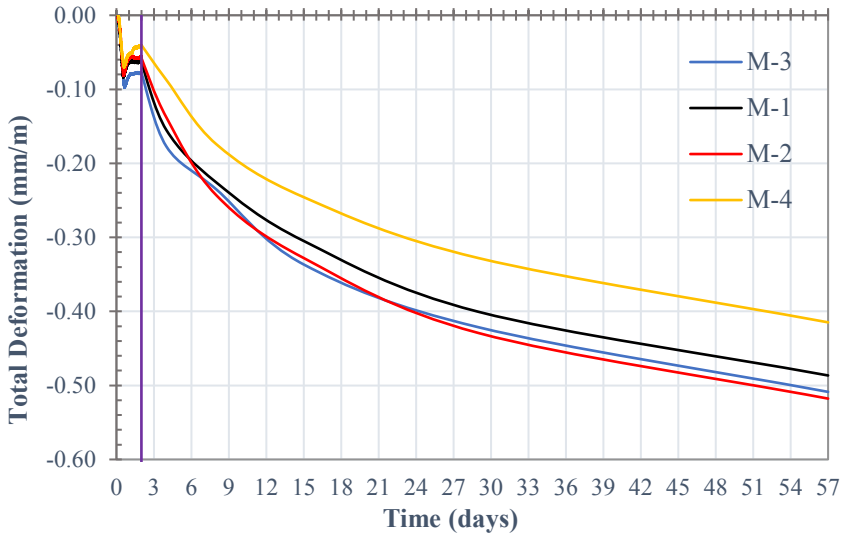

Figure 33 Comparison of Total Deformation (mm/m) of Plus cement concrete mixtures at w/c ratio of 0.50. M1-Plain concrete, M2-Steel fibre concrete, M3-Plastic fibre concrete and M4-Steel fibre concrete with 1% SRA.

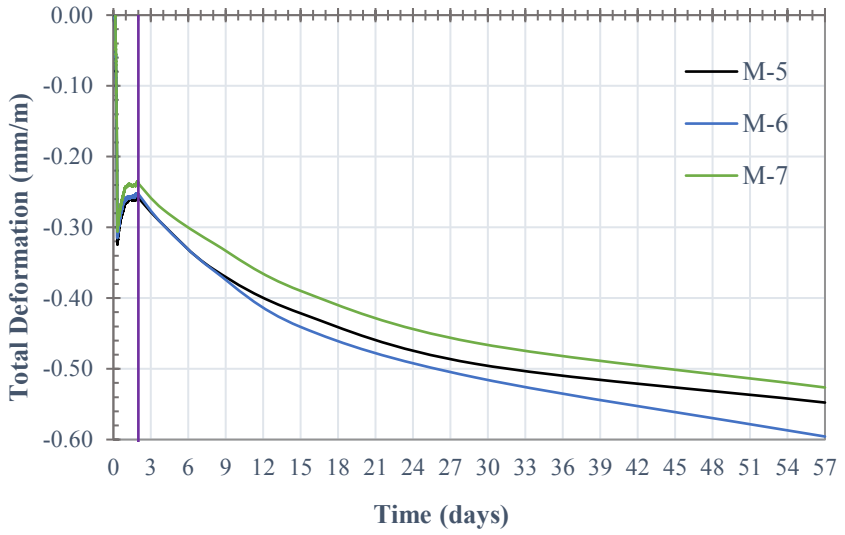

Figure 34 Comparison of Total Deformation (mm/m) of White cement concrete mixtures at w/c ratio of 0.55. M5-Plain concrete, M6-Plastic fibre concrete, M7-Glass fibre concrete.

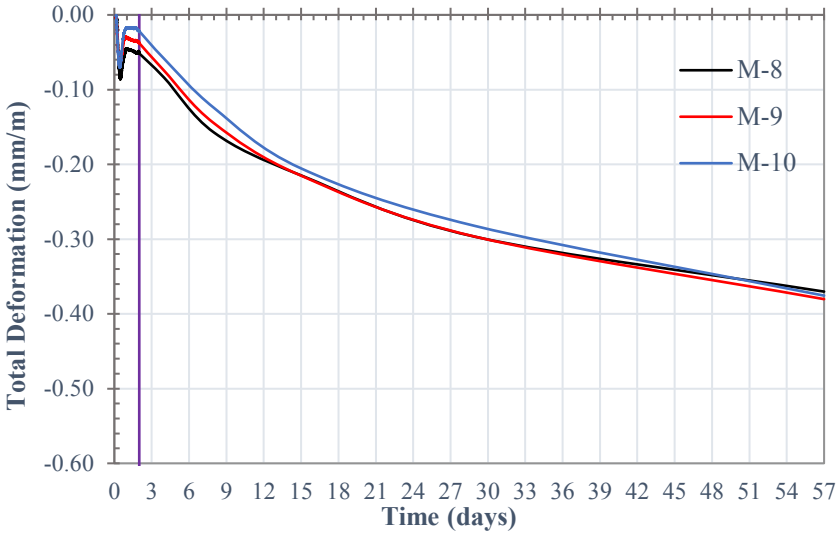

Figure 35 Comparison of Total Deformation (mm/m) of SR cement concrete mixtures at w/c ratio of 0.50. M8-Plain concrete, M9-Steel fibre concrete, M10-Plastic fibre concrete.

A vertical purple line divides the early-age deformation from the long-term drying shrinkage in the Figures 33, 34 and 35. The initial reading for the un-restrained axial drying shrinkage (Section 4.4.2.1) was taken 1 day after demolding and 2 days after production. Therefore, the long-term drying shrinkage values appear from day 2 (the purple line) in this representation of total deformation. Only the absolute magnitude of the drying shrinkage is plotted from where the early-age deformations ended. This approach was adopted because the two experimental setups (bending-drain and shrinkage beams) were separate in their approach. Furthermore, this combined representation of results does not imply the effect of one experimental setup over the other. Due to a large number of variables involved, it is difficult to draw any deductions of the influence of one kind of deformation on the overall results. However, the early-age autogenous deformations are equally important to the long-term drying shrinkage because the concrete is weak and susceptible to cracking at an early age.

The early-age (2-days) autogenous deformation represented approximately 19%, and 22% and 51% of the total combined deformations. From these results, it can be stated that the white cement concrete has the most early-age deforming potential of all three types of cement concretes.

6 Conclusions and Recommendations

The autogenous deformation is of great concern since concretes with lower w/c ratios are more commonly used in applications such as high performance concrete. With material optimization for structural concrete, autogenous deformation is of increasing concern as it can dictate the quality of concrete throughout the lifecycle of a structure. Fibre reinforced cement composites are increasingly being used to address the problems of volumetric deformation-induced cracking. This experiment work was aimed to identify the beneficial effects of fibres in controlling the forces that drive both the early-age autogenous and long-term drying shrinkage deformations in concrete composites. A new experimental setup was used to study the effects of different types of fibers in concrete mixtures with different cement types.

Externally or internally induced shrinkage stresses may lead to cracking if tensile forces exceed the tensile capacity of concrete, either at an early or at a later age. Cracks may occur due to any type of shrinkage deformation phenomenon. The concrete shrinkage phenomenon produces cracks if not countered or relaxed, and reduce the durability of the concrete structure. The autogenous shrinkage deformation measured for different concrete mixtures of 0.50 and 0.55 w/c ratio varied in the magnitude. Water present in the pores of the concrete mixture is internally consumed as the concrete samples were sealed in the bending-drain shrinkage rig. Most of early age autogenous deformation was observed in first 24–hour duration. After 12 to 14 hours, in all cement type mixtures, the deformation was relatively lesser than before. This is the time when concrete hardens and gains enough to resist the driving forces of autogenous deformation. Within the first 12 to 14 hours, large thermal heating-controlled deformations were also observed, followed by a period of thermal cooling in Plus and SR cement concrete mixtures. This indicates the danger of thermal cracking in the fresh concrete.

Different phases of deformation were observed in all the bending-drain experiments for early age autogenous deformation. These phases correspond to various stages of hydration reaction. A comprehensive description of the data interpretation for autogenous shrinkage is presented in Section 5.1.1. The tests for autogenous deformation started approximately 40 minutes after mixing of water with dry materials. After reabsorption of the bleed water and end of thermal swelling, deformation comprised of mostly self-desiccation as the samples were covered and moisture exchange was prevented. Drying shrinkage deformation of hardened concrete (demolding after 24–hour) was measured by a standard shrinkage–beam test in a control room of temperature 20 ^{o}C and RH 65%.

Following trends are concluded from the tests of early age autogenous and long-term drying shrinkage deformation in this study:

- The early age autogenous deformation of plain concrete samples was more than fibre-reinforced samples for all cement types. The fibre dosage of 0.38% by volume was found to be effective in reducing the effects of early age autogenous shrinkage deformations.
- For the same dosage of fibres (0.38% by volume), the plastic (polypropylene) fibres were more effective than hooked-end steel fibres in reducing the early age autogenous shrinkage deformations.
- The effect of fibres in reducing early age autogenous deformation in White cement concrete was less than the effect of fibres addition in Plus and SR cement concrete mixtures.
- Regarding the effect of cement type, the SR cement concrete exhibited both lesser early-age autogenous deformation and long-term drying shrinkage as compared to the Plus cement concrete. This effect is attributed to the difference in clinker composition of the respective cement types. Plus type cement, with a higher C_3A showed greater early age autogenous and long-term drying shrinkage deformation.

- The use of 1% by weight of cement of the Shrinkage Reducing Admixture (SRA) proved to be effective in reducing the early age autogenous and long-term drying shrinkage deformation.
- With little or no bleed water, White cement concrete mixtures exhibited maximum early age autogenous shrinkage deformation and highest rate of temperature rise. This shows that bleed water reabsorption offsets the buildup of pore capillary suction and counters self-desiccation in Plus and SR cement mixtures.
- The 0.38% by volume dosage of fibres had little or no effect on the long-term drying shrinkage in this work. Contrary to some published literature, fibres did not have any pronounced effect on the water loss rate (average water loss expresses in kg/m^3) of hardened concrete beam samples.
- The magnitude of early age autogenous shrinkage deformation was much lesser than long-term drying shrinkage deformation for Plus and SR cement concretes.
- Early age autogenous deformation can be addressed through the design of concrete mixture, which minimizes the autogenous deformations. These factors include cement type (clinker composition, added inert material and fineness), use of shrinkage controlling fibres and use of shrinkage reducing admixtures.

Many factors affect the early age autogenous and long-term drying shrinkage deformations. With regard to the results of this study, following suggestions are made for future studies:

- White cement has a high potential for early age autogenous shrinkage deformation compared to Plus and SR cement. Future work on white cement concrete could focus on the early age deformation characteristics.
- The scope of this study limited the w/c ratio of all the mixtures to explore the behavior of different fibre types. The w/c ratio controls the amount of bleed-water and requirement for superplasticizer, and as such becomes an important factor in the study of early age and long-term deformations.
- The use of SRA in steel fibre plus cement concrete was found to be effective in reducing both the early age (48 hours) and long-term (56 days) drying shrinkage deformations by 37% and 17% respectively. The effect of SRA on fresh properties of concrete and strength properties of concrete should be further studied.
- The temperature history data of different cement type concretes exhibited different nature of hydration kinetics. Thermal heating and cooling during the cement hydration also had an effect on the early age autogenous deformations. Moreover, long-term drying shrinkage of Plus, SR and White cement mixtures differed from each other. For similar concrete composition, the effect of cement type on overall early age and long-term deformations should be studied in more detail.

References

Abbas, Y. M. & Khan, M. I., 2016. Fibre-matrix interactions in fibre-reinforced concrete: A review. *Arabian Journal for Science and Engineering,* Volume 41, pp. 1183-1198.

Afroughsabet, V., Biolzi, L. & Ozbakkaloglu, T., 2016. High-performance fibre-reinforced concrete: a review. *Journal of mateiral scinece,* Volume 51, pp. 6517-6551.

Alvaredo, A. M., 1993. Stability and crack formation under hygral gradients.. *Numerical Models in Fracture Mechanics of Concrete.,* pp. 251-263.

Alvaredo, A. M. & Wittmann, F. H., 1995. Srhinkage and cracking of normal and high performance concrete.. *High Performance Concrete: Material Properties and Design,* pp. 91-110.

Aly, T., Sanjayan, J. G. & Collins, F., 2008. Effect of polypropylene fibres on shrinkage and cracking of concretes. *Materials and Structures,* 41(10), pp. 1741-1753.

ArcelorMittal, 2010. *ds.arcelormittal.com.* [Online] Available at: http://ds.arcelormittal.com/wiresolutions/steelfibres/products/hooked_end_fibres_he/language/EN [Accessed January 2017].

Balaguru, P. & Ramakrishnan, V., 1988. Properties of fibre reinforced concrete: workability, behavior under long-term loading and air-void characteristics. *ACI Materals Journal,* 85(3), pp. 189-196.

Banthia, N. & Gupta, R., 2006. Influence of polypropylene fibre geometry on plastic shrinkage cracking in concrete. *Cement and Concrete Research,* 36(7), pp. 1263-1267.

Barcelo, L. et al., 1999. *Linear vs. volumetric autogenous shrinkage measurement: material behaviour or experimental artefact..* s.l., s.n.

Baroghel-Bouny, V., Mainguy, M., Lassabatere, O. & Coussy, O., 1999. Characterization and identification of equilibrium and transfer moisture properties for ordinary and high-performance cementitious materials. *Cement and Concrete Research,* Volume 21, pp. 1225-1238.

Barr, B. & El-Baden, A., 2003. *Shrinkage properties of normal and high strength fibre reinforced concrete.* s.l., s.n., pp. 15-25.

BASF, 2016. *Master Builders Solutions.* [Online] Available at: https://www.master-builders-solutions.basf.fi/fi-fi/products/masterfiber/354 [Accessed January 2017].

Beltzung, F. & Wittmann, F. H., 2005. Role of disjoining pressure in cement based materials. *Cement and Concrete Research,* Volume 35, pp. 2364-2370.

Bjontegaard, O. & Hammer, T. A., 2006. *Volume Changes of Hardening Concrete: Testing and Mitigation.* Lynby, Denmark, RILEM Publications, pp. 109-125.

Brandt, A. M., 2008. Fibre reinforced cement-based (FRC) composites after 40 years of development iin building and civil engineering. *Composite Structures,* Volume 86, pp. 3-9.

Brinker, C. J. & Scherer, G. W., 1990. *Sol-Gel Science: The physics and chemistry of sol-gel processing,* San Diego: Academic Press, Inc..

Bywalski, C., Kaminski, M., Maszczak, M. & Balbus, L., 2015. Influence of steel fibres addition on mechanical and selected rheological properties of steel fibre high-strength reinforced concrete. *Archives of Civil and Mechanical Engineering,* 15(3), pp. 742-750.

Chanvillard, G. et al., 2009. *Concrete compositon with reduced shrinkage.* US, Patent No. PCT/IB2007/003741.

Chen, P. W. & Chung, D. L., 1996. Low-drying-shrinkage concrete containing carbon fibres. *Compos B Eng,* 27(3), pp. 269-274.

Choi, S. Y., Park, J. S. & Jung, W. T., 2011. *A study on the shrinkage control of fiber reinforced concrete pavement.* s.l., s.n., pp. 2815-2822.

Chuan, J. & Young, C. H., 1990. Study of factors influencing drying shrinkage of steel fibre reinforced concrete. *ACI Materials Journal,* 87(2), pp. 123-139.

Churaev, N. V. & Derjaguin, B. V., 1985. Inclusion of structural forces in the theory of stability of colloids and films. *Journal of Colloid and Interface Science,* 103(2), pp. 542-553.

DiFrancia, C., Ward, T. C. & Claus, R. O., 1996. The single-fibre pull-out test. 1: Review and interpretation. *Composites: Part A 27A,* pp. 597-612.

Eik, M. & Puttonen, J., 2011. Challenges of steel fibre reinforced concrete in load bearing structures. *Journal of Structural Mechanics,* 44(1), pp. 44-64.

El-Aryan, E., 1995. *An investigation of selected material properties of fibre reinforced cellular concrete,* Miami: Univeristy of Miami.

Eppers, S. & Mueller, C., 2008. *Autogenous shrinakge and time-zero of UHPC determined with shrinakge cone.* Ise-Shima, Japan, s.n., pp. 709-714.

Finnsementti Oy, 2016. *www.finnsementti.fi.* [Online] Available at: http://www.finnsementti.fi/en/products/cements [Accessed January 2017].

G, S., Rajabipour, F., Lura, P. & Weiss, J., 2006. *Examining time-zero and early age expansion in pastes containing shrinkage reducing admixtures (SRA'S).* Quebec city, s.n.

Harding, M. A., 1996. *Concrete construction.* [Online] Available at: http://www.concreteconstruction.net/how-to/materials/mixing-placing-and-finishing-fiber-reinforced-concrete_o [Accessed 20 February 2017].

Holt, E. E., 2000. Where did these cracks come from?. *Concrete International,* 22(9), pp. 57-60.

Holt, E. E., 2001. Early age autogenous shrinkage of concrete.

Hua, C., Acker, P. & Ehrlacher, A., 1995. Analyses and models of the autogenous shrinkage of hardening cement paste. *Cement and Concrete Research,* 25(7), pp. 1457-1468.

Inoue, M., Aquino, C., Miura, H. & Okamoto, T., 2010. Influence of limestone aggregate on strength and drying shrinkage of concrete. *Zairyo/Journal of the Society of Materials Science,* 59(10), pp. 769-774.

International, A. S. o. T. M., 2008. *Standard practice for use of apparatus for the determination of length change of hardened cement paste, mortar and concrete,* s.l.: ASTM International.

Janz, M., 2000. *Moisture transport and fixation in porous materials at high moisture levels,* Lund: s.n.

Jenq, Y. S. & Shah, S. P., 1986. Crack Propagation in fibre-reinforced concrete. *Journal of Structural Engineering,* 112(1), pp. 13-34.

Justnes, H., Van Gemert, A., Verboven, F. & Sellevold, E. J., 1996. Total and external chemical shrinkage of low w/c ratio cement pastes. *Advances in Cement Research,* 8(31), pp. 121-126.

Kaikea, A., Achoura, D., Duplan, F. & Rizzuti, L., 2014. Effect of mineral admixtures and steel fibre volume contents on the behavior of high performance fibre reinforced concrete. *Materials & Design,* Volume 63, pp. 493-499.

Kamen, A., 2006. *Time dependent behavior of ultra high performance fibre reinforced concrete.* Zurich, s.n.

Katzer, J. & Domski, J., 2012. Quality and mechanical properties of engineered steel fibres used as reinforcement for concrete. *Construction and Building Materials,* Volume 34, pp. 243-248.

Kell, G. S., 1975. Volume properties of ordinary water. *Journal of Chemical & Engineering Data,* Volume 12, pp. 67-68.

Kinuthia, J. M., Wild, S., B., B. & Bai., J., 2000. Self-compensating autogenous shrinkage in portland cement-metakaolin-fly ash pastes. *Advances in Cement Research,* 12(1), pp. 35-43.

Kosmatka, S. & Panarese, W., 1988. *Design and control of concrete mixtures,* Skokie: Portland Cement Association.

Kovler, J. & Bentur, A., 1997. Shrinkage of early age steel fibre reinforced concrete. *Archives of Civil Engineering,* XLIII(4), pp. 431-439.

Kovler, K., Sikuler, J. & Bentur, A., 1992. *Free and restrained shrinkage of fibre reinforced concrete with low polypropylene fibre content at early age.* Sheffield, RILEM, pp. 91-101.

Kucharczykova, B. et al., 2017. Comprehensive Testing Techniques for the Measurement of Shrinkage and Structural Changes of Fine-Grained Cement-Based Composites during Ageing.. *Advances in Materials Science and Engineering,* Volume 2017.

Lei, Y. & Cao, X., 2011. Study on thermal dilaiton coefficient of fibre concrete at early stage. *Applied Mechanics and Materials,* Volume 99-100, pp. 777-781.

Lura, P. et al., 2007. Influence of shrinkage-reducing admixtures on development of plastic shrinakage cracks.. *ACI Materials Journal,* 104(2), pp. 187-194.

Mangat, P. S. & Azari, M. M., 1984. A theory for the free shrinkage of steel fibre reinforced cement matrices. *Journal of Material Sciences,* 19(7), pp. 2183-2194.

Mehta, P. K. & Monteiro, P. J., 2006. *Concrete: Microstructure, Properties, and Materials.* New York: McGraw-Hill.

Mindess, S. & Young, J. F., 1981. *Concrete,* s.l.: Prentice-Hall, Inc..

Myers, D., Kang, T. H. & Ramseyer, C., 2008. Early-age properites of polymer fibre-reinforced concrete. *ACI Materials Journal,* 2(1), pp. 9-14.

Neville, A. M. & Brooks, J. J., 2010. *Concrete Technology.* Second ed. Malaysia: Pearson Education Limited.

Owens Corning, 2015. *Owens Corning - Innovations for Living.* [Online] Available at: http://www.cem-fil.com/ [Accessed January 2017].

Padron, I. & Zollo, R. F., 1990. Effect of synthetic fibres on volume stability and cracking of portland cement concrete and mortar. *ACI Materials Journal,* 87(4), pp. 327-332.

Paillere, A. M., Buil, M. & Serrano, J. J., 1989. Effect of fibre addition on autogenous shrinkage of silica fume concrete. *ACI Materials Journal,* 86(2), pp. 139-144.

Paulini, P., 1996. *Outlines of hydraulic hardening - an energetic appraoch.* New Delhi, India, s.n.

Pemat, 1985. *Pemat.* [Online] Available at: http://www.pemat.de/produkte/mischer/gleichlaufmischer/zz-75-he/ [Accessed January 2017].

Radocea, A., 1992. *A study on the mechanism of plastic shrinkage of cement-based materials,* Goteborg: s.n.

Roziere, E., Delsaute, B., Loukili, A. & Staquet, S., 2015. *Experimental assessment of autogenous shrinkage.* Vienna, s.n.

Ruacho, J. M., Gettu, R. & Aguado, A., 2009. Influence of shrinkage-reducing admixture on the reduction of plastic shrinkage cracking in concrete.. *Cement and Concrete Research,* Volume 39, pp. 141-146.

Saje, D. et al., 2012. Autogenous and drying shrinkage of fibre reinforced high-performance cocnrte. *Journal of Advanced Concrete Technology,* Volume 10, pp. 59-73.

Saje, D., Lopatic, J. & Saje, F., 2003. The influence of concrete ingredients on shrinkage of high performance concrete. *Journal o fthe Mechancial Behavior of Materials,* 14(2), pp. 173-182.

Sandbakk, S., 2007. *Influence of fibres on cracking due to plastic and drying shrinkage,* Trondheim: SINTEF Building and Infrastructure.

Schleibinger Geräte, 2015. *Schleibinger Testing Systems.* [Online] Available at: http://www.schleibinger.com/cmsimple/en/?Shrinkage:Bending_Drain [Accessed January 2017].

Shah, H. R. & Weiss, J., 2006. Quantifying shrinkage cracking in fibre reinforced concrete using the ring test. *Materials and Structures,* Volume 39, pp. 887-899.

Sivakumar, A. & Santhanam, M., 2007. A quantitative study on the plastic shrinkage cracking in high strength hybrid fribre reinforced concrete. *Cement and Concrete Composites,* 29(7), pp. 575-581.

Sun, W., Chen, H., Luo, X. & Qian, H., 2001. The effect of hybrid fibers and expansive agent on the shrinkage and permeability of high-performance concrete. *Cement and Concrete Research,* 31(4), pp. 595-601.

Swamy, R. N. & Stavrides, H., 1979. Influence jof fibre reinforcement on restrained shrinkage and cracking. *ACI Journal,* 76(3), pp. 443-460.

Tanaka, H. & Hashida, H., 2009. *Effect of limestone as aggregate on reducing drying shrinkage of concrete.* Ise-Shima, Japan, Taylor & Francis Group, pp. 877-883.

Tazawa, E.-i. & Miyazawa, S., 1995. Influence of cement and admixture on autogenous shrinkage of cement paste.. *Cement and Concrete Research,* 25(2), pp. 281-287.

Tazawa, E.-i., Ryoichi, S., Sakai, E. & Miyazawa, S., 2000. Work of JCI committee on autogenous shrinkage. In: *PRO 17: international RILEM Workshop on Shrinkage of concrete - 'Shrinkage 2000'.* Paris: s.n., pp. 21-40.

VonFay, K. F., Morency, M., Bissonnette, B. & Vaysburd, A. M., 2009. *Development of test methods to evaluate cracking tendency of repair materials - field study - phase II,* s.l.: Concrete repair engineering experimental program (CREEP).

Wittmann, F. H., 1975. On the action of capillary pressure in fresh concrete. *Cement and concrete research,* 6(1), pp. 49-56.

Wittmann, F. H., 1985. Deformation of concrete at variable moisture content. *Mechancis of Geomaterials,* pp. 425-459.

Wittmann, F. H., Beltzung, F. & Zhao, T.-J., 2009. Shrinkage mechanicms, crack formation and service life of reinforced cocnrete structures. *International Journal of Structural Engineering,* 1(1).

Woyciechowski, P., Chilmon, K. & Sokolowska, J. J., 2016. *Effect of limestone and granite coarse aggregate on drying shrinkage of a concrete.* Moscow, MATEC Web of Conferences.

Zollo, R. F., 1975. Fibre reinforced concrete extrusions. *Journal of Structural Division,* 101(12), pp. 2573-2583.

Zollo, R. F., 1984. *Collated fibrillated polypropylene fibres in FRC.* s.l., American Concrete Institute, pp. 397-409.

Zollo, R. F., 1996. Fibre-reinforced concrete: an overview after 30 years of development. *Cement and Concrete Composites,* Volume 19, pp. 107-122.

Zollo, R. F., Ilter, J. A. & Bouchacourt, G. B., 1986. *Plastic and drying shrinkage in concrete containing collated fibrillated polypropylene fibres.* Cachan, France, RILEM Technical Committee 49-TFR.

Appendix 1 (1/1): Standards

Experimental work done in this research followed the practices mentioned in the following standards parts either partially or completely. For reference, brief explanation is presented corresponding to the standard name.

- SFS EN 12617–4(2002): Products and systems for the protection and repair of concrete structures–Test methods–Part4: Determination of shrinkage and expansion.
  The European Standard explains a method for measuring the shrinkage and expansion deformation controlled by the variation of moisture content in the hydraulic cement composites as defined by EN1504–1.
- ISO1920–8:2009(E): Testing of concrete – Part 8: Determination of drying shrinkage of concrete for samples prepared in the filed or in the laboratory.
  The International Standard specifies a method for determining axial length changes of prismatic concrete specimens due to drying in air, and the method of sample preparation and curing for the same specimens for which the maximum aggregate may not exceed 25 mm.
- PrEN13892–9:2017(E): Methods of test for screed materials–Part 9: Determination of shrinkage and swelling.
  This draft European Standard specifies a method for determining the deformation (shrinkage and swelling) of cementitious screed, calcium sulfate screed, magnesite screed and synthetic resin screed materials made in accordance with EN13892–1.
- EN12350–2:2009: Testing fresh concrete–Part2: Slump–test.
  This European standard specifies a method for the determination of consistence of fresh concrete by measuring the slump for concretes with maximum aggregate size less than 40 mm.
- EN12350–7:2009: Testing fresh concrete–Part7: Air content–Pressure methods.
  This standard describes two method for determination of air content of compacted fresh concrete, made with normal weight or relatively dense aggregate of maximum size 63 mm.